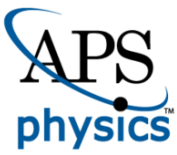

Entanglement-preserving approach for reservoir-induced photonic dissipation in waveguide QED systems

Zihao Chen, Yao Zhou, and Jung-Tsung Shen

Phys. Rev. A **98**, 053830 — Published 19 November 2018

DOI: 10.1103/PhysRevA.98.053830

Entanglement-preserving Approach for Reservoir-induced Photonic Dissipation in Waveguide QED Systems

Zihao Chen, Yao Zhou, and Jung-Tsung Shen*

Department of Electrical and Systems Engineering,

Washington University in St. Louis, Missouri 63130, USA

(Dated: October 23, 2018)

Abstract

Using an entanglement-preserving approach, we theoretically study the reservoir-induced photonic dissipations in waveguide quantum electrodynamic (wQED) systems coupled to an excitable reservoir consisting of oscillators. For the single-photon case, we show that the effects of dissipation can be described by a reduced Hamiltonian and a restricted eigenstate. For the multi-photon case, we show that the reduced Hamiltonian approach is, in general, not valid. Nonetheless, we identify a weak-reservoir condition for the reduced Hamiltonian approach to be approximately valid, which applies to the majority of current experiments. In addition, we apply the density matrix approach to investigate the same physical system, and show that the Markovian density matrix approach can describe only the lowest-order dissipative effect. The deviations from the weak-reservoir scenario are suggested to be observable in an engineered excitable reservoir consisting of optical cavities.

* jushen@wustl.edu

I. INTRODUCTION

The interactions between the microscopic constituents of a physical system fundamentally lead to the quantum entanglement between the constituent parts. Often, due to either computational constraints or physical considerations, we restrict ourselves simply to the quantum states of the part of the physical system of interest and average out the degrees of freedom of the residual parts. For example, when solving a quantum-mechanical problem of the spontaneous decay of an excited atom, or the problem of the decay of the radiation field inside a cavity with partially transparent mirrors, what we really do is divide the entire physical system into two parts–the part of the system of interest (henceforth will simply be called 'system' for brevity) and the rest of the system (which is also called the environment or the reservoir) with a large number of degrees of freedom [1, 2]. As a consequence, a dissipation (damping) term emerges in the system which characterizes the leakage rate of particle or energy from the system to the reservoir.

Conventionally, a very fruitful approach to studying the effects of dissipation is the density matrix approach. Such an approach traces over the environmental degrees of freedom and phenomenologically parametrizes the system-environment interaction as damping terms in the Lindblad superoperators in the resultant quantum master equation for a dissipative system [2, 3]. The detailed information of the system-environment entanglement is eliminated at the very beginning in the density matrix approach. As a result, the density matrix approach provides a probabilistic measure for the system evolutions in terms of mixed states. Another aspect is that, as the density matrix approach does not include the wave function of the photon field, the photon-atom entanglement can not be directly described. Other successful approaches include the quantum Langevin approach, which is also widely used to investigate the dissipation-driven fluctuation and temporally-correlated statistics [4]; and the quantum jump approach which has been developed for statistical single-photon loss processes [5] and can be numerically simulated using the Monte-Carlo techniques [6]. The limitations of the density matrix approach with regard to the entanglement also apply to the quantum Langevin and the quantum jump approaches.

Recently, an entanglement-preserving approach [7] is adopted to treat the problem of reservoir-induced dissipation when the environment is non-excitable (e.g., a vacuum or a homogeneous transparent medium) [8]. The explicit example considered is the reservoir-

induced dissipation of a two-level atom in a waveguide QED (wQED) system with an input of quantized optical field. The atom is coupled to an optical waveguide and a reservoir that is a homogeneous, three-dimensional, non-excitable, photonic space with infinitely many photonic scattering channels. It is shown that, for an input of an arbitrary photonic Fock state or a coherent state, the dissipative dynamics of the system can be described by reduced Hamiltonian (i.e., adding a renormalized term and an imaginary part $-i\gamma$ in the atomic transition frequency) and a restricted eigen-state which are restricted to the Hilbert space of the wQED system only (i.e., omitting the scattering channels of the environment in the wavefunction). That is, the dissipation rate γ due to the reservoir can be measured by a single-photon scattering experiment (e.g., a transmission measurement); the resulting reduced Hamiltonian is then valid for all quantized optical input.

In this article, we apply this approach to investigate the wQED system of the same configuration as that in Ref. [8], but now instead with an *excitable* reservoir that consists of infinitely many quantum oscillators. Such a scenario is ubiquitous in practical photonic systems (e.g., free-carrier absorption in highly-doped semiconductor waveguide [9], absorption-driven cladding loss in photonic crystal fiber [10], and generic material absorption in other silica-based photonic devices [11, 12]), and has been of great theoretical and experimental interest to the studies of the quantum dynamics of many cavity and waveguide QED systems [13–23]. Throughout the approach, the entanglements between each constituent parts (photons, the two-level atom, and the reservoir oscillators) are explicitly retained. It is found that in this scenario the reduced Hamiltonian description is valid only when the input is a single-photon Fock state, and breaks down when the input field contains more than one photons. Specifically, we found that for an N-photon Fock state input ($N > 1$), the reduced Hamiltonian description remains valid for the eigen-state describing the uncorrelated plane waves of photons. For all these cases (single-photon input and uncorrelated photons), the reduced Hamiltonian is straightforwardly obtained by replacing the transition frequency Ω of the two-level system with the renormalized complex transition frequency $\bar{\Omega} = \Omega + \alpha$ in the system Hamiltonian. The real part and the imaginary part of the complex $\alpha = \Delta\Omega - i\gamma$ describe the shift of the transition frequency and the dissipation rate, respectively, due to coupling to the excitable reservoir. The expression of α is shown to be identical for all uncorrelated states and a closed form for α is derived, which involves summing over all admissible closed trajectories of the leaking photons hopping among the oscillators in the reservoir.

Nonetheless, for correlated eigen-states describing the bound states of photons [24] and the hybrid states (which are product states of the plane waves and bound states, see Ref. [25] for classification details), the reduced Hamiltonian description is no longer valid. The reason for breaking down is due to the presence of the photonic correlations in these states: When the reservoir is excitable, the escaped photons from the system to the reservoir have a chance to be scattered back to the system and thus change the existing correlations. In contrast, in the non-excitable reservoir case [8], after being dissipated, the photon can never come back to the system. Finally, we also carry out the calculation using the density matrix approach and show that the result obtained from the Markovian density matrix approach is the lowest order of α obtained using the entanglement-preserving approach. Our findings indicate that the dissipation rate γ obtained from the single-photon scattering experiments in general cannot be directly used to account for the multi-photon dynamics. In the weak-reservoir limit when the couplings to and within the reservoir is weak, the correlated eigenstates can otherwise be described by a reduced Hamiltonian, and both the entanglement-preserving approach and the density matrix approach yield the same results.

This article is organized as follows. In Sec. II, we introduce the physical model to describe the microscopic material loss mechanism (Henceforth, we shall call the dissipation induced by the non-excitable reservoir the scattering loss and by the excitable reservoir the material loss.) In Sec. III, we investigate the effects of the reservoir for the single-photon case, and validate the reduced Hamiltonian approach. Then, in Sec. IV and Sec. V, we study the two-photon and the arbitrary N-photon Fock state cases. In addition, we also derive the weak-reservoir conditions for the reduced Hamiltonian approach to be approximately valid. In Sec. VI, we apply the density matrix approach to investigate the material loss model, and compare the results with those of our entanglement-preserving approach. Finally, in Sec. VII, we draw conclusions and provide an outlook for our work.

II. MODEL AND HAMILTONIAN

The physical wQED system considered is shown schematically in Fig. 1. The system (S) consists of a two-level atom coupled to a single-mode photonic waveguide, and an N-photon Fock state, $|N\rangle$, is injected into the waveguide from the left. The incoming photons interact with the atom through absorptions, spontaneous, and stimulated emission processes. On the

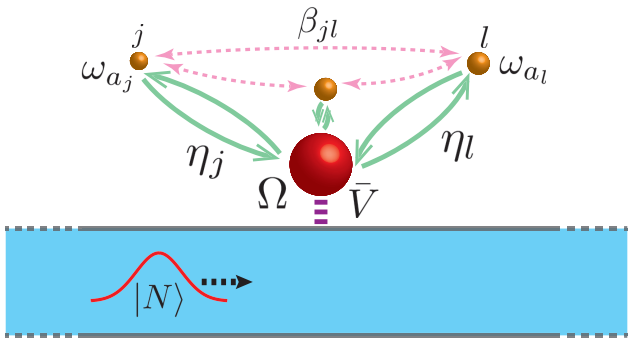

FIG. 1. Schematics of the waveguide QED system with an excitable reservoir. A two-level atom (represented by a red sphere) is coupled to the one-dimensional single-mode photonic waveguide. The atom is further coupled to a reservoir that consists of infinitely many excitable oscillators (represented by yellow dots). j and l are indices of any two oscillators ($j, l = 1, 2, \cdots$). Ω and ω_a denote transition frequencies for the atom and the oscillators, respectively. $\bar{V}$, η, and β are the atom-photon, atom-oscillator, and the inter-oscillator coupling strengths, respectively. $|N\rangle$ denotes the incoming N-photon Fock state.

other hand, due to the coupling between the atom and the external excitable oscillators, the photon may leak out to the reservoir and undergo secondary scattering processes between the oscillators. The Hamiltonian describing the wQED system in Fig. 1, H_S, is

$$\begin{aligned}\frac{H_S}{\hbar} = \int dx \Big\{ & c_R^\dagger(x)(-iv_g\partial_x)c_R(x) + c_L^\dagger(x)(iv_g\partial_x)c_L(x) \\ & + \bar{V}\delta(x)[(c_R^\dagger(x) + c_L^\dagger(x))\sigma_- + \sigma_+(c_R(x) + c_L(x))]\Big\} \\ & + \omega_e a_e^\dagger a_e + \omega_g a_g^\dagger a_g,\end{aligned} \tag{1}$$

where the linear dispersion approximation and the rotating-wave approximation are employed [7]. $c_R^\dagger(x)$ ($c_R(x)$) denotes the creation (annihilation) operator for a right-moving photon at position x. $c_L^\dagger(x)$ and $c_L(x)$ are similarly defined for a left-moving photon. $a_g^\dagger$ (a_g) denotes the creation (annihilation) operator for the atomic ground state with energy $\hbar\omega_g$. $a_e^\dagger$ and ω_e are similarly defined for the atomic excited state. $\Omega \equiv \omega_e - \omega_g$ is the atomic transition frequency. $\sigma_+ = a_e^\dagger a_g$ ($\sigma_- = a_g^\dagger a_e$) is the atomic raising (lowering) operator. v_g denotes the group velocity of photons in the waveguide. $\bar{V}$ is the atom-photon coupling

strength. The Hamiltonian describing the reservoir, H_R, is given by

$$\begin{aligned}\frac{H_R}{\hbar} =& \sum_j \left[(\omega_{e_j} - i\varepsilon) a_{e_j}^\dagger a_{e_j} + \omega_{g_j} a_{g_j}^\dagger a_{g_j}\right] \\ &+ \sum_{j,l,j\neq l} \frac{\beta_{jl}}{2} \left(\sigma_{j+}\sigma_{l-} + \sigma_{l+}\sigma_{j-}\right),\end{aligned} \tag{2}$$

where $a_{g_j}^\dagger$ (a_{g_j}) denotes the creation (annihilation) operator for the ground state of the j-th oscillator with energy $\hbar\omega_{g_j}$ ($j = 1, 2, \cdots$); $a_{e_j}^\dagger$, a_{e_j}, and ω_{e_j} are similarly defined for its excited state; and $\omega_{a_j} \equiv \omega_{e_j} - \omega_{g_j}$ is the transition frequency of the j-th oscillator. $\sigma_{j+} = a_{e_j}^\dagger a_{g_j}$ ($\sigma_{j-} = a_{g_j}^\dagger a_{e_j}$) denotes the raising (lowering) operator for the j-th oscillator. β_{jl} represents the inter-oscillator coupling strength between the j-th and the l-th oscillators. In the following, a general description is provided without imposing special constraints on the functional form of β_{jl}'s, thus allowing the incorporation of various scenarios. For example, the value of β_{jl} can decrease as the separation between the the j-th and the l-th oscillators increases according to a specified fashion so that only short-ranged hops make contributions. Each oscillator has an intrinsic scattering loss rate ε, which is taken to be 0^+ at the end of the calculation to ensure the causality condition. It is worth noting that albeit only frequency and inter-oscillator coupling of the reservoir are considered, our approach can readily incorporate more reservoir degrees of freedom (e.g., mode, polarization, spin, intrinsic scattering loss, and etc). The Hamiltonian describing the system-reservoir coupling, H_{SR}, is

$$\frac{H_{SR}}{\hbar} = \sum_j \eta_j \left(\sigma_{j+}\sigma_- + \sigma_+\sigma_{j-}\right), \tag{3}$$

where η_j is the coupling strength between the atom and the j-th oscillator. The Hamiltonian describing the combined system $S \oplus R$ (wQED system + reservoir), H, is given by $H_S + H_R + H_{SR}$.

III. SINGLE-PHOTON CASE

We first study the case of the excitable reservoir for the case of single-photon input. The general single-photon eigenstate of the combined system, $|\Phi_1\rangle$, is

$$|\Phi_1\rangle = \Big(\int dx \left[\phi_R(x) c_R^\dagger(x) + \phi_L(x) c_L^\dagger(x)\right] + e\sigma_+ + \sum_j \phi_j \sigma_{j+} \Big) |\varnothing\rangle, \tag{4}$$

where ϕ_R (ϕ_L) denotes the right- (left-) moving single-photon wave function. e and ϕ_j denote the excitation amplitude for the atom and the j-th oscillator, respectively. $|\varnothing\rangle$ is the

photonic vacuum state that has no waveguided photons; the atom is in the ground state; and none of the oscillators are excited. By applying Schrödinger Equation $H|\Phi_1\rangle = \hbar\tilde{\epsilon}|\Phi_1\rangle$, where $\hbar\tilde{\epsilon} = \hbar(\omega_k + \omega_g + \sum_j \omega_{g_j})$ is the total energy of the combined system with $\hbar\omega_k$ being the energy of the incident photon, and equating the coefficients for each basis, the equations of motion are obtained as follows,

$$\omega_k \phi_R(x) = -iv_g \partial_x \phi_R(x) + V\delta(x)e, \tag{5a}$$

$$\omega_k \phi_L(x) = iv_g \partial_x \phi_L(x) + V\delta(x)e, \tag{5b}$$

$$\omega_k e = V\left[\phi_R(0) + \phi_L(0)\right] + \Omega e + \sum_j \eta_j \phi_j, \tag{5c}$$

$$\omega_k \phi_j = (\omega_{a_j} - i\varepsilon)\phi_j + \eta_j e + \sum_{l,l\neq j} \beta_{jl}\phi_l. \tag{5d}$$

Note that Eq. (5d) can be rearranged as

$$\phi_j = \frac{\eta_j}{(\omega_k - \omega_{a_j} + i\varepsilon)} e + \frac{1}{(\omega_k - \omega_{a_j} + i\varepsilon)} \sum_{l,l\neq j} \beta_{jl}\phi_l. \tag{6}$$

From Eq. (6), ϕ_j can be solved for recursively and yields the following expression

$$\begin{aligned} \phi_j = \Big(&\frac{\eta_j}{\omega_k - \omega_{a_j} + i\varepsilon} + \sum_{l,l\neq j} \frac{\beta_{jl}\eta_l}{(\omega_k - \omega_{a_j} + i\varepsilon)(\omega_k - \omega_{a_l} + i\varepsilon)} \\ &+ \sum_{l,l\neq j} \sum_{m,m\neq l} \frac{\beta_{jl}\beta_{lm}\eta_m}{(\omega_k - \omega_{a_j} + i\varepsilon)(\omega_k - \omega_{a_l} + i\varepsilon)(\omega_k - \omega_{a_m} + i\varepsilon)} + \cdots \Big) e. \end{aligned} \tag{7}$$

In each term of ϕ_j, the numerator describes a path of the photons hopping between the oscillators and the two-level atom with an increasing length. For example, the first term denotes a one-hop path of the photon jumping from the j-th oscillator directly to the two-level atom, while the second term describes a two-hop path of the photon jumping from the j-th oscillator to an intermediate l-th oscillator ($l \neq j$) and then to the two-level atom. By plugging the expression of ϕ_j (Eq. (7)) into Eq. (5c), Eq. (5c) now reads as

$$\begin{aligned} &\omega_k e = V\left[\phi_R(0) + \phi_L(0)\right] + (\Omega + \alpha)e, \quad \text{where} \\ &\alpha = \sum_{n=1}^{\infty} \alpha_n, \quad \alpha_1 = \sum_{i_1} \frac{\eta_{i_1}^2}{\omega_k - \omega_{a_{i_1}} + i\varepsilon}, \\ &\alpha_n = \sum_{i_1} \sum_{i_2, i_2\neq i_1} \cdots \sum_{i_n, i_n \neq i_{n-1}} \frac{\eta_{i_1}\beta_{i_1 i_2}\cdots\beta_{i_{n-1}i_n}\eta_{i_n}}{\prod_{l=1}^{n}(\omega_k - \omega_{a_{i_l}} + i\varepsilon)}, \quad n = 2, 3, \cdots. \end{aligned} \tag{8}$$

Note that for each α_n, the numerator describes a closed path of the photon, starting from the two-level atom (the η_{i_1} term) and hopping $n-1$ times between the oscillators in the

reservoir (the β's terms), and eventually ending with the two-level atom (the η_{i_n} term). The real part and the imaginary part of the complex frequency renormalization $\alpha = \Delta\Omega - i\gamma$ describe the shift of the transition frequency of the two-level atom and the dissipation rate, respectively, due to coupling to the excitable reservoir. Fig. 2 provides a graphic representation of the numerators of α_n. The returning nature of the single-photon paths has a far-reaching consequence for the correlated multi-photon transport, as the returning times are statistical and generally breaks down the photonic temporal entanglement within the waveguide.

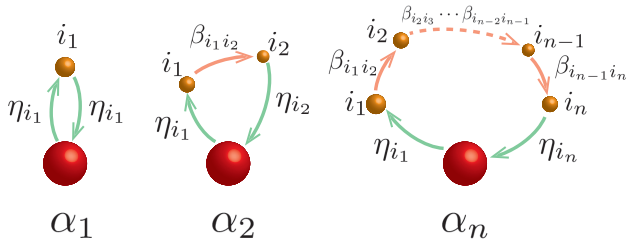

FIG. 2. Graphic representation of the complex frequency renormalization $\alpha \equiv \sum_n \alpha_n$: for each α_n, the numerator describes a closed path of the photon, staring from the two-level atom (η) and hopping $n-1$ times between the oscillators in the reservoir (β's), and finally ending with the two-level atom (η).

Together, Eqs. (5a), (5b), and (8) now form a set of self-consistent equations which only involve the system amplitudes ϕ_R, ϕ_L, and e. Such a result states that after taking into account the statistical fluctuations of the system-reservoir coupling (*i.e.*, η) and the secondary scattering characteristic of the reservoir (*i.e.*, β), the wave function information of ϕ_j can be traced over and incorporated in the renormalized frequency $\bar{\Omega} \equiv \Omega + \alpha$ ($\alpha \equiv \sum_{n=1}^{\infty} \alpha_n$). That is, the combined system can be described by a reduced Hamiltonian (substituting Ω with the renormalized transition frequency $\bar{\Omega}$ in the system Hamiltonian H_S), and a restricted eigenstate $|\Phi_1\rangle = (\int dx \left[\phi_R(x) c_R^\dagger(x) + \phi_L(x) c_L^\dagger(x)\right] + e\sigma_+)|\varnothing\rangle$ which contains only the degrees of freedom of the system.

For an ensemble of oscillators with closely spaced frequencies that form a quasi-continuous frequency distribution (which occurs even for identical oscillators due to, for example, heterogeneous local conditions), we can convert the n-th order renormalization α_n ($n = 1, 2, \cdots$) from the discrete expression to the continuum case as follows: the discrete frequency ω_{a_j} is replaced by the continuous frequency variable ω_j; the discrete-valued function $\beta_{i_m i_l}$ and

η_{i_l} now become functions of continuous frequency variables, $\beta(\omega_m, \omega_l)$ and $\eta(\omega_l)$, respectively; and the discrete summation $\sum_{i_l}$ is replaced by the integral of continuous frequency distribution $\int d\omega_l D(\omega_l)$, where D denotes the density of states in the reservoir.

Here, we first make coarse approximations for the magnitude of α_j to gain insights. When the relevant variables change slowly with respect to the frequency, the integrals can be approximated by using the average values that are independent of the frequency. That is, η, D, and β are approximated by $\bar{\eta}$, $\bar{D}$, and $\bar{\beta}$, respectively; $\omega_k - \omega + i\varepsilon$ is approximated by the average atom-reservoir detuning $\bar{\delta}$; and the integral $\int d\omega$ can be approximated by multiplying an average reservoir bandwidth $\Delta\omega$. By plugging such approximations in Eq. (8), one has that $\alpha_j \approx \bar{\eta}^2 \bar{\beta}^{j-1} \bar{D}^j \Delta\omega^j / \bar{\delta}^j$ $(j = 1, 2, \cdots)$. Apparently, when $\alpha_{j+1}/\alpha_j = \bar{\beta}\bar{D}\Delta\omega/\bar{\delta} \ll 1$, dissipative effects that are described by terms of orders higher than one can be neglected. That is, α can be approximated by its lowest-order term α_1 when a combined condition of weak secondary scattering strength, low density of states, narrow reservoir bandwidth, and large photon-reservoir detuning, *i.e.*, $\bar{\beta}\bar{D}\Delta\omega/\bar{\delta} \ll 1$, is satisfied.

For the continuum case, the first-order and second-order renormalizations α_1 and α_2 take the following forms (hereafter, we shall assume that the incoming photon is intune with the atom $\omega_k \approx \Omega$, which is the typical case of interest in practice):

$$\begin{aligned} \alpha_1 &= \int d\omega_1 \frac{\eta^2(\omega_1) D(\omega_1)}{\Omega - \omega_1 + i\varepsilon}, \\ \alpha_2 &= \iint\limits_{\omega_1 \neq \omega_2} d\omega_1 d\omega_2 \frac{\beta(\omega_1, \omega_2)\eta(\omega_1)\eta(\omega_2) D(\omega_1) D(\omega_2)}{(\Omega - \omega_1 + i\varepsilon)(\Omega - \omega_2 + i\varepsilon)}. \end{aligned} \tag{9}$$

By invoking the Sokhotski-Plemelj (S-P) theorem, (*i.e.*, $\lim\limits_{\varepsilon \to 0^+} 1/(\omega - \omega_1 + i\varepsilon) = P[1/(\omega - \omega_1)] - i\pi\delta(\omega - \omega_1)$, P denotes the Cauchy principal value), and the Poincaré-Bertrand (P-B) formula (*i.e.*, $P\frac{1}{X-Y}P\frac{1}{X-Z} = P\frac{1}{Y-Z}(P\frac{1}{X-Y} - P\frac{1}{X-Z}) + \pi^2\delta(X-Y)\delta(X-Z)$), it follows that

$$\begin{aligned} &\alpha_1 = \Delta_1 - i\gamma_1, \alpha_2 = \Delta_2 - i\gamma_2, \quad \text{where} \\ &\Delta_1 = P\int d\omega_1 \frac{\eta^2(\omega_1) D(\omega_1)}{\Omega - \omega_1}, \quad \gamma_1 = \pi\eta^2(\Omega) D(\Omega), \\ &\Delta_2 = P\iint d\omega_1 d\omega_2 \frac{f(\omega_1, \omega_2)}{\omega_1 - \omega_2}\left(\frac{1}{\Omega - \omega_1} - \frac{1}{\Omega - \omega_2}\right), \\ &\gamma_2 = \pi\left[P\int d\omega_2 \frac{f(\Omega, \omega_2)}{\Omega - \omega_2} + P\int d\omega_1 \frac{f(\omega_1, \Omega)}{\Omega - \omega_1}\right], \\ &f(\omega_1, \omega_2) = \beta(\omega_1, \omega_2)\eta(\omega_1)\eta(\omega_2) D(\omega_1) D(\omega_2), \end{aligned} \tag{10}$$

where Δ_1 and γ_1 represent the resulting first-order transition frequency shift, and the first-order intrinsic dissipation rate, respectively. Δ_2 and γ_2 are similarly defined for the second-order terms. By recursively applying the S-P theorem and the P-B formula, higher-order frequency renormalizations $\alpha_n = \Delta_n - i\gamma_n$ can also be obtained, where Δ_n and γ_n are the n-th order transition frequency shift and dissipation rate, respectively ($n = 3, 4, \cdots$). Noting that the first-order renormalization only involves the system-reservoir interaction while the second-order term provides further information on the inter-oscillator interaction in the reservoir. Then, by defining the collective transition frequency $\Delta = \sum_{n=1}^{\infty} \Delta_n$, and the collective dissipation rate $\gamma = \sum_{n=1}^{\infty} \gamma_n$, α now reads as $\alpha = \Delta - i\gamma$. As a result, the effect of the reservoir manifests as a transition frequency shift Δ, and an intrinsic dissipation rate γ.

To summarize the single-photon case, we show explicitly that the effects of the reservoir can be described by a reduced Hamiltonian (with a renormalized frequency $\Omega \to \bar{\Omega} = \Omega + \Delta - i\gamma$ in H_S), and a restricted eigenstate ($|\Phi_1\rangle = (\int dx \left[\phi_R(x)c_R^\dagger(x) + \phi_L(x)c_L^\dagger(x)\right] + e\sigma_+)|\varnothing\rangle$). To simplify the notations, in the above derivation we have assumed that all η's and β's are real-valued. The general case when these variables are complex numbers can be straightforwardly obtained in the same manner.

IV. TWO-PHOTON CASE

Having solved the single-photon dynamics in the presence of the reservoir, we now study the case when the input is a two-photon Fock state. Specifically, we will first solve the equations of motion for the two-photon dynamics for the interacting eigenstates of the Hamiltonian for the restricted system variables (*i.e.*, omitting the degrees of freedom in the reservoir). We then apply the Lippmann-Schwinger formalism to obtain the corresponding in- and out- states to construct the *restricted* scattering matrix, which will be denoted as $\mathbf{S}^r$. As the restricted Hamiltonian is not hermitian, consequently, the restricted scattering matrix $\mathbf{S}^r$ is not unitary. For the dissipationless two-photon case when no reservoir is present, it has been shown that the two-photon plane-wave states alone do not form a complete set of two-photon eigenstates of the scattering matrix, and a two-photon bound state must be included for the completeness [24, 26]. We now examine the effects of the reservoir for the plane-wave states and the bound state solutions separately. (See Ref. [26] and [25] for detailed

procedures for the two- and N-photon case, respectively, when no reservoir is present).

A. Hamiltonian and Equations of Motion

As a first step, it is mathematically convenient to convert the Hamiltonian H to that in the even mode (H_e) and that in the odd mode (H_o, $H = H_e + H_o$) such that H_e and H_o are decoupled ($[H_e, H_o] = 0$). H_o is an interaction-free chiral Hamiltonian, while H_e describes a nontrivial, interacting chiral Hamiltonian. Since the photon-atom interactions are encoded in the even mode, not the odd mode, we will focus on the even-mode physics hereafter. The transformation of the wavefuctions and the S-matrix from the even and odd chiral modes to the physical two-mode case has been investigated [26].

By invoking the operator transformations, $c_e^\dagger(x) = [c_R^\dagger(x) + c_L^\dagger(-x)]/\sqrt{2}$ and $c_o^\dagger(x) = [c_R^\dagger(x) - c_L^\dagger(-x)]/\sqrt{2}$, one obtains the following even-mode Hamiltonian H_e describing the combined system,

$$\begin{aligned}\frac{H_e}{\hbar} =& \int dx \left\{ c_e^\dagger(x)(-iv_g\partial_x)c_e(x) + V\delta(x)\left[c_e^\dagger(x)\sigma_- + \sigma_+ c_e(x)\right]\right\} \\ &+\omega_e a_e^\dagger a_e + \omega_g a_g^\dagger a_g + \sum_j \eta_j \left(\sigma_{j+}\sigma_- + \sigma_+\sigma_{j-}\right) \\ &+\sum_j \left((\omega_{e_j} - i\varepsilon) a_{e_j}^\dagger a_{e_j} + \omega_{g_j} a_{g_j}^\dagger a_{g_j} \right) \\ &+\sum_{j,l,j\neq l} \frac{\beta_{jl}}{2}\left(\sigma_{j+}\sigma_{l-} + \sigma_{l+}\sigma_{j-}\right),\end{aligned} \tag{11}$$

where $c_e^\dagger(x)$ ($c_e(x)$) is the operator to create (annihilate) a photon at position x in the even mode. $V = \sqrt{2}\bar{V}$ is the atom-photon coupling strength in the even mode. The general form of the two-photon interacting eigenstate of the combined system, $|\Phi_2\rangle$, is given by

$$\begin{aligned}|\Phi_2\rangle =& \Big(\iint dx_1 dx_2 \phi(x_1,x_2)\frac{1}{\sqrt{2}} c_e^\dagger(x_1)c_e^\dagger(x_2) \\ &+ \int dx e(x) c_e^\dagger(x)\sigma_+ + \sum_j \int dx \phi_j(x) c_e^\dagger(x)\sigma_{j+} \\ &+ \sum_j e_j \sigma_+\sigma_{j+} + \sum_{j,l,j<l} e_{jl}\sigma_{j+}\sigma_{l+}\Big)|\varnothing\rangle,\end{aligned} \tag{12}$$

where $\phi(x_1, x_2)$ denotes the wave function for two waveguided photons in the even mode. Due to the boson statistics, the wave function satisfies $\phi(x_1, x_2) = +\phi(x_2, x_1)$, and is continuous on the line $x_1 = x_2$. $e(x)$ is the probability amplitude distribution of one waveguided photon

while the atom in the excited state. $\phi_j(x)$ denotes the probability amplitude distribution of one waveguided photon while the j-th oscillator in the excited state. e_j represents the excitation amplitude wherein two photons are absorbed by the atom and the j-th oscillator, respectively. e_{jl} is the excitation amplitude wherein two photons are absorbed by the j-th and the l-th oscillators, respectively. By applying the Schrödinger Equation, $H_e|\Phi_2\rangle = \hbar\tilde{\epsilon}|\Phi_2\rangle$, one obtains the following equations of motion,

$$\begin{aligned}\epsilon\phi(x_1,x_2) =& -iv_g\left(\partial_{x_1}+\partial_{x_2}\right)\phi(x_1,x_2)\\ &+\frac{V}{\sqrt{2}}\left[\delta(x_1)e(x_2)+\delta(x_2)e(x_1)\right],\end{aligned} \tag{13a}$$

$$\begin{aligned}\epsilon e(x) =& -iv_g\partial_x e(x)+\frac{V}{\sqrt{2}}\left[\phi(0,x)+\phi(x,0)\right]\\ &+\Omega e(x)+\sum_j \eta_j\phi_j(x),\end{aligned} \tag{13b}$$

$$\begin{aligned}\epsilon\phi_j(x) =& -iv_g\partial_x\phi_j(x)+V\delta(x)e_j+(\omega_{a_j}-i\varepsilon)\phi_j(x)\\ &+\eta_j e(x)+\sum_{l,l\neq j}\beta_{jl}\phi_l(x),\end{aligned} \tag{13c}$$

$$\begin{aligned}\epsilon e_j =& V\phi_j(0)+\sum_{l,l<j}\eta_l e_{lj}+\sum_{l,l>j}\eta_l e_{jl}\\ &+\left(\omega_a+\omega_{a_j}-i\varepsilon\right)e_j+\sum_{l,l\neq j}\beta_{jl}e_l,\end{aligned} \tag{13d}$$

$$\begin{aligned}\epsilon e_{jl} =& \eta_j e_l+\eta_l e_j+\left(\omega_{a_j}+\omega_{a_l}-2i\varepsilon\right)e_{jl}+\sum_{m,m\neq l,m<j}\beta_{lm}e_{mj}\\ &+\sum_{m,m\neq l,m>j}\beta_{ml}e_{jm}+\sum_{m,m\neq j,m<l}\beta_{jm}e_{ml}+\sum_{m,m\neq j,m>l}\beta_{mj}e_{lm},\end{aligned} \tag{13e}$$

where $\hbar\epsilon = \hbar(\tilde{\epsilon}-\omega_g-\sum_j\omega_{g_j})$ gives the total energy of two photons.

Our computational strategy is as follows. We will solve Eqs. (13a), (13b), and (13c) to obtain the solution of the interacting eigenstate of H_e for the variables restricted in the system of interest (*i.e.*, $\phi(x_1,x_2)$ and $e(x)$). In particular, we will show that the wavefunctions of the reservoir degrees of freedom (*i.e.*, $\phi_j(x)$, e_j, and e_{jl}) can be traced over, and have no direct relevance to our results, which is similar to the single-photon case. Thus, in the end, Eqs. (13d) and (13e) are not directly involved in the calculation. The two-photon in- and out- states can be constructed based upon the interacting eigenstates for restricted system variables (*i.e.*, $|\Phi_2\rangle = \Big(\iint dx_1dx_2\phi(x_1,x_2)c_e^\dagger(x_1)c_e^\dagger(x_2)/\sqrt{2}+\int dxe(x)c_e^\dagger(x)\sigma_+\Big)|\varnothing\rangle$), and further normalized to obtain eigenstates of the restricted scattering matrix.

B. Two-photon Plane-wave Solution for Excitable Reservoir Case

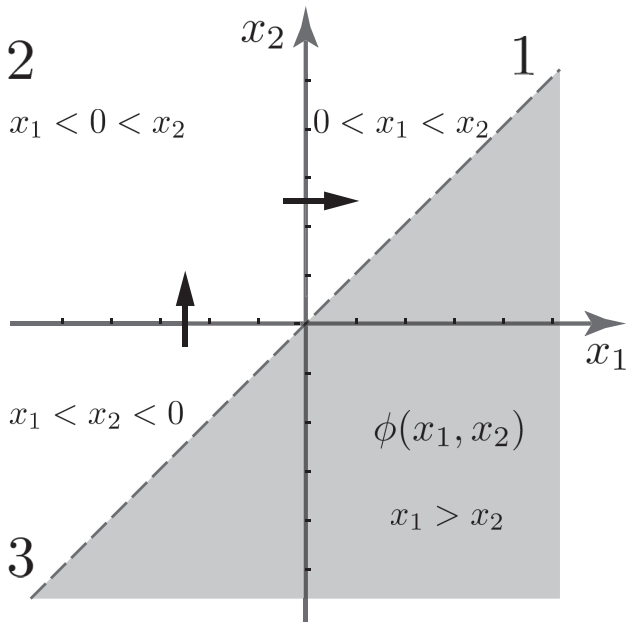

FIG. 3. The *divide and conquer* scheme to solve the two-photon interacting eigenstates. Due to bosonic symmetry, only half of the entire x_1-x_2 coordinate plane (*i.e.*, $x_1 < x_2$) is involved in the calculation. The x_1-axis, the x_2-axis, and the $x_1 = x_2$ line further dissect the half plane into three regions, *i.e.*, Region 1 ($0 < x_1 < x_2$), 2 ($x_1 < 0 < x_2$), and 3 ($x_1 < x_2 < 0$). When given $\phi(x_1, x_2)$ in Region 3, the boundary condition is imposed to obtain $\phi(x_1, x_2)$ in other regions, as indicated by the arrows.

We first focus on the two-photon plane-wave solution when the waveguide is coupled to an excitable reservoir. Due to bosonic symmetry of photon wave functions, we only consider the solution of $\phi(x_1, x_2)$ for half of the entire x_1-x_2 plane. Without loss of generality, we will focus on the $x_1 < x_2$ half plane, which is further sub-divided into three ordered regions: Region 1 ($0 < x_1 < x_2$); 2 ($x_1 < 0 < x_2$); and 3 ($x_1 < x_2 < 0$), as indicated in Fig. 3. Note that the photon-atom interactions occur only on the two coordinate axes of $x_1 = 0$ and $x_2 = 0$. Region 3 and 1 correspond to the wave functions wherein two photons are both on the left of the atom (*i.e.*, before scattering), and both on the right of the atom (*i.e.*, after scattering), respectively; Region 2 corresponds to the case wherein one photon is on the right of the atom while the other photon on the left. Following the Bethe Ansatz, the

two-photon plane-wave solution takes the following form,

$$\phi(x_1,x_2)=\begin{cases} B_3 e^{i\frac{\omega_k}{v_g}x_1+i\frac{\omega_p}{v_g}x_2}+A_3 e^{i\frac{\omega_k}{v_g}x_2+i\frac{\omega_p}{v_g}x_1}, & \text{in Region 3,}\\ B_2 e^{i\frac{\omega_k}{v_g}x_1+i\frac{\omega_p}{v_g}x_2}+A_2 e^{i\frac{\omega_k}{v_g}x_2+i\frac{\omega_p}{v_g}x_1}, & \text{in Region 2,}\\ B_1 e^{i\frac{\omega_k}{v_g}x_1+i\frac{\omega_p}{v_g}x_2}+A_1 e^{i\frac{\omega_k}{v_g}x_2+i\frac{\omega_p}{v_g}x_1}, & \text{in Region 1.}\end{cases} \tag{14}$$

ω_k and ω_p denote the angular frequencies of two photons, respectively. We adopt the *divide and conquer* scheme to solve for $\phi(x_1,x_2)$ (*i.e.*, the amplitudes A's and B's) in the $x_1<x_2$ half plane, in the order of Region $3\to 2\to 1$, as indicated by the arrows in Fig. 3, which corresponds to a pictorial representation of the scattering process.

Applying the equations of motions on the boundaries between adjacent Region 2 and 3 gives rise to the following boundary condition for $x<0$,

$$\phi(x,0^+)=\phi(x,0^-)-i\frac{V}{\sqrt{2}v_g}e(x). \tag{15}$$

By plugging Eq. (15) into Eq. (13b), one has that

$$\begin{aligned}-iv_g\partial_x e(x)=&\left(\epsilon-\Omega+i\frac{\Gamma}{2}\right)e(x)\\ &-\sqrt{2}V\phi(x,0^-)-\sum_j \eta_j\phi_j(x),\end{aligned} \tag{16}$$

where $\Gamma=V^2/v_g$ is the atomic decay rate into the waveguide in the even mode. The general solution of Eq. (16) for $x<0$ is

$$\begin{aligned}e(x)=&c_o e^{\frac{i}{v_g}(\epsilon-\Omega+i\frac{\Gamma}{2})x}+\frac{i}{v_g}e^{\frac{i}{v_g}(\epsilon-\Omega+i\frac{\Gamma}{2})x}\\ &\int_{-\infty}^{x}dx' e^{-\frac{i}{v_g}(\epsilon-\Omega+i\frac{\Gamma}{2})x'}[-\sqrt{2}V\phi(x',0^-)-\sum_j\eta_j\phi_j(x')],\end{aligned} \tag{17}$$

where c_o is a constant to be determined. To determine c_o, we note that when the atom is decoupled from the waveguide (*i.e.*, $V=0$), neither the atom nor any oscillator can be excited, thus leading to $e(x)=0$ and $\phi_j(x)=0\ \forall x$. As a result, one obtains $c_o=0$. In addition, $\phi_j(x)$ for $x<0$ takes the following general form,

$$\phi_j(x)=c_j e^{i\frac{\omega_k}{v_g}x}+d_j e^{i\frac{\omega_p}{v_g}x}. \tag{18}$$

By plugging Eq. (18) and $\phi(x,0^-)|_{x<0}=B_3e^{i\omega_k x/v_g}+A_3e^{i\omega_p x/v_g}$ into Eq. (17), one obtains $e(x)$ for $x<0$,

$$e(x)=\frac{\sqrt{2}VB_3(1+\xi_B)e^{i\frac{\omega_k}{v_g}x}}{\omega_p-\Omega+i\frac{\Gamma}{2}}+\frac{\sqrt{2}VA_3(1+\xi_A)e^{i\frac{\omega_p}{v_g}x}}{\omega_k-\Omega+i\frac{\Gamma}{2}}, \tag{19}$$

where $\xi_A \equiv \sum_j d_j\eta_j/\sqrt{2}VA_3$, $\xi_B \equiv \sum_j c_j\eta_j/\sqrt{2}VB_3$ are defined for brevity. To eliminate ξ_A and ξ_B, one now further plugs Eq. (19) into Eq. (13c) to obtain $\phi_j(x)$ for $x < 0$, which takes the following form

$$\begin{aligned}\phi_j(x) =&\frac{\eta_j\sqrt{2}VB_3(1+\xi_B)}{(\omega_p-\Omega+i\frac{\Gamma}{2})(\omega_p-\omega_{a_j}+i\varepsilon)}e^{i\frac{\omega_k}{v_g}x}\\ &+\frac{\sum_{l,l\neq j}\beta_{jl}c_l}{(\omega_p-\omega_{a_j}+i\varepsilon)}e^{i\frac{\omega_k}{v_g}x}\\ &+\frac{\eta_j\sqrt{2}VA_3(1+\xi_A)}{(\omega_k-\Omega+i\frac{\Gamma}{2})(\omega_k-\omega_{a_j}+i\varepsilon)}e^{i\frac{\omega_p}{v_g}x}\\ &+\frac{\sum_{l,l\neq j}\beta_{jl}d_l}{(\omega_k-\omega_{a_j}+i\varepsilon)}e^{i\frac{\omega_p}{v_g}x}.\end{aligned} \tag{20}$$

By equating Eq. (18) and Eq. (20), c_j and d_j can be determined. Specifically, c_j is given by

$$c_j =\frac{\eta_j}{(\omega_p-\omega_{a_j}+i\varepsilon)}f+\frac{\sum_{l,l\neq j}\beta_{jl}c_l}{(\omega_p-\omega_{a_j}+i\varepsilon)}, \tag{21}$$

where $f \equiv \sqrt{2}VB_3(1+\xi_B)/(\omega_p-\Omega+i\Gamma/2)$. Similar to Eqs. (6) and (7), c_j can be solved for recursively and expressed in terms of f as follows

$$\begin{aligned}c_j =&\Big(\frac{\eta_j}{\Omega-\omega_{a_j}+i\varepsilon}+\sum_{l,l\neq j}\frac{\beta_{jl}\eta_l}{(\Omega-\omega_{a_j}+i\varepsilon)(\Omega-\omega_{a_l}+i\varepsilon)}\\ &+\sum_{l,l\neq j}\sum_{m,m\neq l}\frac{\beta_{jl}\beta_{lm}\eta_m}{(\Omega-\omega_{a_j}+i\varepsilon)(\Omega-\omega_{a_l}+i\varepsilon)(\Omega-\omega_{a_m}+i\varepsilon)}+\cdots\Big)f,\end{aligned} \tag{22}$$

where the intune condition $\omega_p \approx \Omega$ is assumed here, the same as in the single-photon case. (d_j can be analogously derived and shown to have a similar expression, which is not detailed here.) Note that the terms in the parentheses in Eq. (22) are identical to those in Eq. (7), the excitation amplitude for the oscillators. Consequently, by substituting Eq. (22) into the summation $\sum_j c_j\eta_j$, one obtains $\sum_j c_j\eta_j = \alpha f$, where α here is identical to the frequency renormalization obtained in the single-photon case (Eq. (8)). By further plugging $\sum_j c_j\eta_j$ into ξ_B, one obtains $\xi_B = \alpha(1+\xi_B)/(\omega_p-\Omega+i\Gamma/2)$. With such explicit form of ξ_B, the coefficient of $e^{i\omega_k x/v_g}$ in Eq. (19) can be simplified such that the factor $(1+\xi_B)/(\omega_p-\Omega+i\Gamma/2)$ now reduces to $1/(\omega_p-\Omega+i\Gamma/2-\alpha)$. By performing similar calculations for the $e^{i\omega_p x/v_g}$ term, Eq. (19) now reads as

$$e(x) =\sqrt{2}VB_3\frac{e^{i\frac{\omega_k}{v_g}x}}{\omega_p-\bar{\Omega}+i\frac{\Gamma}{2}}+\sqrt{2}VA_3\frac{e^{i\frac{\omega_p}{v_g}x}}{\omega_k-\bar{\Omega}+i\frac{\Gamma}{2}}, \tag{23}$$

where $\bar{\Omega} = \Omega + \alpha = \Omega + \Delta - i\gamma$ is the renormalized transition frequency that is the same as the single-photon case. Having solved $e(x)$ for $x < 0$, we now follow the *divide and conquer* scheme to obtain $\phi(x_1, x_2)$ in Region 2. By applying the boundary condition between Region 2 and 3, when $x < 0$, one obtains

$$\begin{aligned}\phi(x, 0^+) =& \phi(x, 0^-) - i\frac{V}{\sqrt{2}v_g}e(x) \\ =& \bar{t}_p B_3 e^{i\frac{\omega_k}{v_g}x} + \bar{t}_k A_3 e^{i\frac{\omega_p}{v_g}x},\end{aligned} \tag{24}$$

where $\bar{t}_{k,p} = (\omega_{k,p} - \bar{\Omega} - i\Gamma/2)/(\omega_{k,p} - \bar{\Omega} + i\Gamma/2)$. Note that the single-photon transmission coefficient in reservoir-free case is given by $t_{k,p} = (\omega_{k,p} - \Omega - i\Gamma/2)/(\omega_{k,p} - \Omega + i\Gamma/2)$. Thus, $\bar{t}_k$ and $\bar{t}_p$ are the renormalized single-photon transmission coefficients that can be described by the same frequency renormalization $\Omega \to \bar{\Omega}$. By equating Eq. (24) and $\phi(x, 0^+)|_{x<0} = B_2 e^{i\omega_k x/v_g} + A_2 e^{i\omega_p x/v_g}$ from Eq. (14), one obtains that $B_2 = \bar{t}_p B_3$ and $A_2 = \bar{t}_k A_3$.

So far, we have laid out the analysis for $e(x)|_{x<0}$, and the relation of amplitudes between Region 2 and 3. Following similar procedures, one can also obtain $e(x)|_{x>0}$, and the relation of amplitudes between Region 1 and 2. As a result, eigen wave functions of the restricted system variables (*i.e.*, $\phi(x_1, x_2)$ and $e(x)$) for the two-photon plane-wave solution is obtained, as summarized in Fig. 4. Note that by invoking the continuous boundary condition for the atomic wave function, *i.e.*, $e(0^-) = e(0^+)$ (deduced from Eq. (13b)), the amplitude relation of $B_3/A_3 = (\omega_p - \omega_k - i\Gamma)/(\omega_p - \omega_k + i\Gamma)$ can be determined. Interestingly, the solutions follow the same form as that in the reservoir-free case (see Fig. 7 in Ref. [26]), yet with a frequency renormalization $\Omega \to \bar{\Omega}$ that is the same as the single-photon case. By using the Lippmann-Schwinger formalism, the solved set of interacting eigenstates for the restricted system variables can be used to construct the in-state $|\text{in}\rangle$ for the two-photon plane-wave solution in the following

$$\begin{aligned}|\text{in}\rangle =& \iint dx_1 dx_2 \phi_{\text{in}}(x_1, x_2) \frac{1}{\sqrt{2}} c_e^\dagger(x_1) c_e^\dagger(x_2) |\varnothing\rangle, \quad \text{where} \\ \phi_{\text{in}}(x_1, x_2) =& \text{Ext}[\phi(x_1, x_2)|_{x_1<x_2<0}], \\ =& \text{Ext}[B_3 e^{i\frac{\omega_k}{v_g}x_1 + i\frac{\omega_p}{v_g}x_2} + A_3 e^{i\frac{\omega_k}{v_g}x_2 + i\frac{\omega_p}{v_g}x_1}],\end{aligned} \tag{25}$$

where Ext denotes the extension of the functional form from the constrained region (*e.g.*, $x_1 < x_2 < 0$ here) to the entire space ($-\infty < x_1, x_2 < \infty$) (see Eqs. (88)-(90) in Ref. [26],

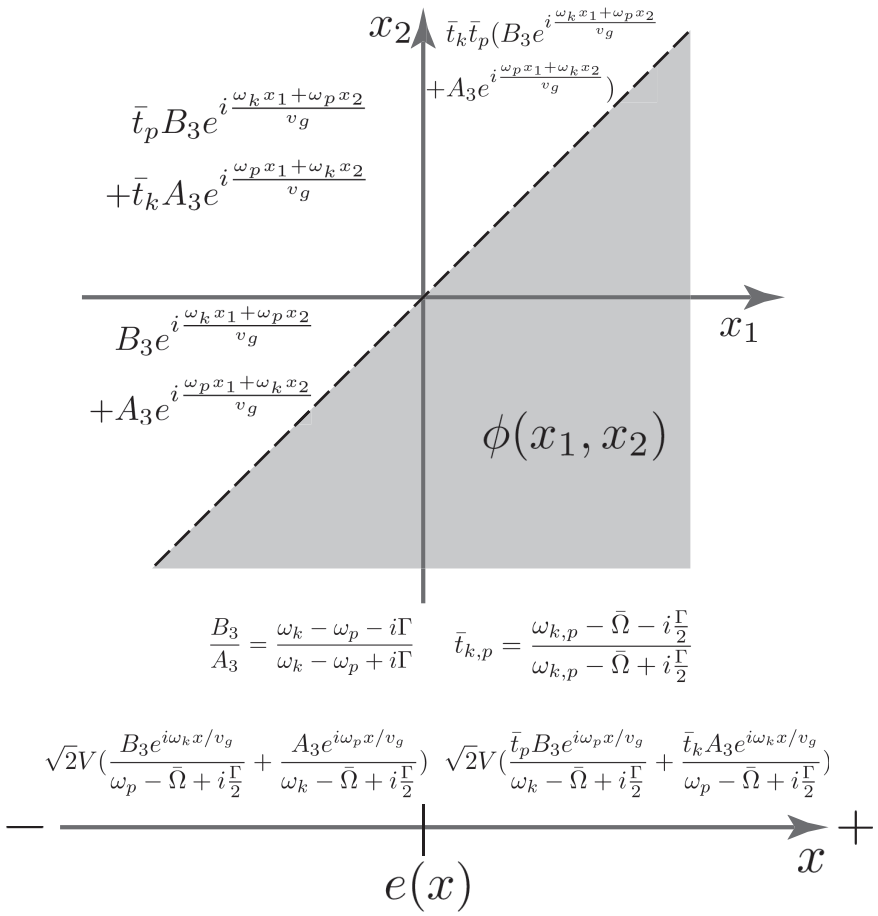

FIG. 4. Interacting eigenstate solution of the restricted system variables $\phi(x_1, x_2)$ and $e(x)$ to Eqs. (13) for the two-photon plane-wave state case. $\phi(x_1, x_2)$ is specified in Region 1, 2, and 3. $e(x)$ is specified for both $x > 0$ and $x < 0$.

and Eqs. (8), (9) in Ref. [25] for detailed derivations). Similarly, the out-state is given by

$$\begin{aligned} |\text{out}\rangle =& \iint dx_1 dx_2 \phi_{\text{out}}(x_1, x_2) \frac{1}{\sqrt{2}} c_e^\dagger(x_1) c_e^\dagger(x_2) |\varnothing\rangle, \quad \text{where} \\ \phi_{\text{out}}(x_1, x_2) =& \text{Ext}[\phi(x_1, x_2)|_{0<x_1<x_2}], \\ =& \text{Ext}[\bar{t}_p\bar{t}_k(B_3 e^{i\frac{\omega_k}{v_g}x_1 + i\frac{\omega_p}{v_g}x_2} + A_3 e^{i\frac{\omega_k}{v_g}x_2 + i\frac{\omega_p}{v_g}x_1})], \end{aligned} \tag{26}$$

Based on the in- and the out-states, one can construct the normalized eigenstate $|W_{k,p}\rangle$ of the restricted even-mode S-matrix, $\mathbf{S}^r_{e^{(2)}}$, in the following form,

$$\begin{aligned} |W_{k,p}\rangle =& \iint dx_1 dx_2 W_{k,p}(x_1, x_2) \frac{1}{\sqrt{2}} c_e^\dagger(x_1) c_e^\dagger(x_2) |\varnothing\rangle, \quad \text{where} \\ W_{k,p}(x_1, x_2) =& \frac{\sqrt{2} e^{iKx_c} [2\Delta \cos \Delta x_d - \kappa \text{sgn}(x_d) \sin \Delta x_d]}{2\pi \sqrt{[4\Delta^2 + \kappa^2]}}, \end{aligned} \tag{27}$$

where $K = \epsilon/v_g$, $x_d = x_1 - x_2$, $x_c = (x_1 + x_2)/2$, $\kappa = \Gamma/v_g$, $\Delta = (\omega_k - \omega_p)/2v_g$ and sgn is the sign function. It can be immediately obtained from the analysis outlined above that $\mathbf{S}^r_{e^{(2)}}|W_{k,p}\rangle = \bar{t}_k\bar{t}_p|W_{k,p}\rangle$. *Here, we note that* $|W_{k,p}\rangle$ *follows exactly the same functional form as that in the reservoir-free case.*

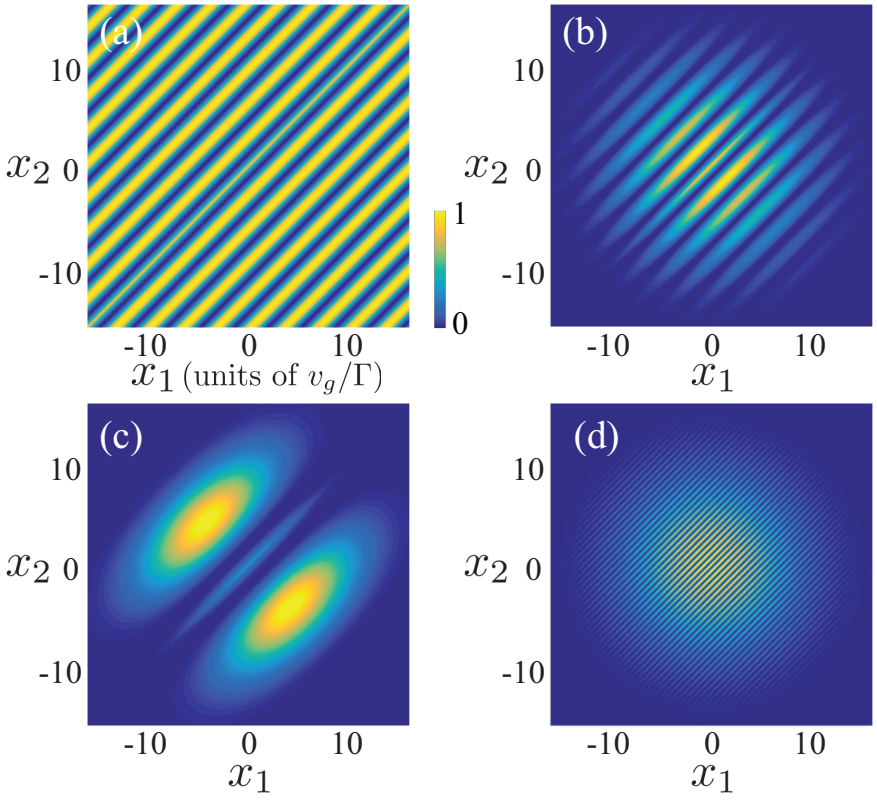

FIG. 5. Density plot for the wavefunction of the two-photon plane-wave state. (a) $|W_{k,p}|^2$ when $\Delta = \kappa$. (b) Gaussian-modulated two-photon plane-wave state $|W^G_{k,p}|^2$ when $\Delta = \kappa$. $|W^G_{k,p}|^2$ is centered at $x_1 = x_2 = x_o = 0$. (c) $|W^G_{k,p}|^2$ when $\Delta = 0.2\kappa$. (d) $|W^G_{k,p}|^2$ when $\Delta = 5\kappa$. For the density plot, the numerical values for one unit scale are (a) 0.25, (b) 0.23, (c) 0.027, and (d) 5 in units of Γ^2/v_g^2 (which has a unit of 1/Length^2).

To visualize the real-space representation of the two-photon plane-wave state, here we plot the wave function density $|W_{k,p}(x_1, x_2)|^2$ in Fig. 5 for the case $\omega_k \neq \omega_p$ ($\Delta \neq 0$). (The density is equal to zero everywhere when $\Delta = 0$.) Fig. 5(a) plots the case of $\Delta = \kappa$, wherein the interference fringes are extended along the diagonal ($x_1 = x_2$), and periodically modulated in the transverse direction ($x_1 = -x_2$). Such a periodic structure results from the fact that given a fixed Δ, $|W_{k,p}|^2$ only depends on the distance between two individual photons, *i.e.*, $x_1 - x_2$, and is modulated by the sinusoidal functions. The spatial period is $\pi/\sqrt{2}\Delta$, and the

corresponding spatial frequency is $2\sqrt{2}\Delta$. The maximal density is $|W_{k,p}|^2_{\max} = 1/2\pi^2$, which is attained when $\Delta x_d = m\pi - \arccos(2\Delta/\sqrt{4\Delta^2+\kappa^2})$ $(m = 0, \pm1, \pm2, \cdots)$. Nonetheless, the density on the $x_1 = x_2$ line does not attain the maximal density, which is equal to only $4\Delta^2/(4\Delta^2+\kappa^2)$ of $|W_{k,p}|^2_{\max}$.

In practice, the two-photon states exist as wavepackets (pulses), which have a finite spatial size and a finite frequency bandwidth. Fig. 5(b) plots the density of the Gaussian-modulated plane-wave state $W^G_{k,p} \equiv W_{k,p} \times \mathcal{M}$, where $\mathcal{M} \equiv \exp[-(x_1-x_o)^2/4\sigma_x^2 - (x_2-x_o)^2/4\sigma_x^2]$ is the modulation function. x_o is the center position of the wave packet. The spatial width of the modulation σ_x is chosen to be $5v_g/\Gamma$ such that the pulse has a narrow bandwidth $\Gamma/10$. $|W^G_{k,p}|^2$ decreases as $|x_1 - x_2|$ increases. Figure 5(c) and (d) plot $|W^G_{k,p}|^2$ for $\Delta = 0.2\kappa$ and $\Delta = 5\kappa$, respectively, wherein the number of fringes reflects the spatial beating frequencies of the two photons.

C. Two-photon Bound State Solution for Excitable Reservoir Case

1. Reservoir-free case:

To fully characterize the two-photon scattering processes requires a complete set of eigenstates of $\mathbf{S}^r_{e^{(2)}}$, which span the free two-photon Hilbert space. For the reservoir-free case, it has been shown that the two-photon plane-wave states $\{|W_{k,p}\rangle, k \le p\}$ do not form a complete set while an additional two-photon bound state $|B_K\rangle$ has to be taken into account for the completeness [24, 26]. The two-photon bound state, $|B_K\rangle = \iint dx_1 dx_2 B_K(x_1,x_2) c^\dagger_e(x_1) c^\dagger_e(x_2)/\sqrt{2}$, is labeled by the total energy ϵ of two photons, or equivalently, the total wave vector $K \equiv \epsilon/v_g$; $B_K(x_1,x_2) = \sqrt{\kappa/4\pi} e^{iKx_c - \kappa|x_1-x_2|/2}$ (see Ref. [24] for the expression of bound state). The properties of the two-photon bound state: (i) $|B_K\rangle$ describes a two-photon bound state as the probability amplitude decays exponentially when the distance between two photons, $|x_1 - x_2|$, increases. (ii) $|B_K\rangle$ is orthogonal to $|W_{k,p}\rangle$, that is, $\langle B_K|W_{k,p}\rangle = 0$, $\forall K$, k, and p. (iii) $|B_K\rangle$ is an eigenstate of the scattering matrix the reservoir-free case. (iv) In momentum space representation, $B_K(k_1,k_2) = \sqrt{\kappa^3/4\pi}\delta(K-k_1-k_2)/[(k_1-K/2)^2+\kappa^2/4]$, where $B_K(k_1,k_2) = \iint dx_1 dx_2 B_K(x_1,x_2) e^{-i(k_1x_1+k_2x_2)}/2\pi$. The Dirac-$\delta$ function here (*i.e.*, $\delta(K-k_1-k_2)$) indicates that in the momentum space, the frequencies of the two photons are anti-correlated.

The two-photon bound state has been experimentally confirmed [27].

2. Reservoir is present:

When an excitable reservoir is present, as is the case here, the set $\{|W_{k,p}\rangle, k \leq p\}$ again do not form a complete set. In the following, we show that *a two-photon bound state exists even when the excitable reservoir is present*. Such a reservoir-modified two-photon bound state has a much more involved expression than the two-photon bound state $|B_K\rangle$ for the reservoir-free case. Before we embark on the detailed mathematical derivation, here we outline the physical reason why $|B_K\rangle$ fails to be an eigenstate in the presence of the reservoir. Similar to the plane-wave state case, we only take into account half of the entire x_1-x_2 plane, *i.e.*, $x_1 < x_2$. The functional form of $B_K(x_1, x_2)$ in Region 3 is given by $\phi(x_1, x_2) \propto e^{i[(Kv_g - i\Gamma)x_1 + (Kv_g + i\Gamma)x_2]/2v_g}$. By applying the *divide and conquer* scheme, one determines the atomic excitation $e(x)$ in the following form

$$
\begin{aligned}
e(x)|_{x<0} =& \sqrt{2}V \frac{e^{\frac{i}{v_g}\frac{Kv_g - i\Gamma}{2}x}}{\frac{Kv_g}{2} - \Omega_+ + i\Gamma}, \\
e(x)|_{x>0} =& \sqrt{2}V \frac{\frac{Kv_g}{2} - \Omega_+}{\frac{Kv_g}{2} - \Omega_-} \frac{e^{\frac{i}{v_g}\frac{Kv_g + i\Gamma}{2}x}}{\frac{Kv_g}{2} - \Omega_+ + i\Gamma}, \quad \text{where} \\
\Omega_\pm =& \Omega + \mu_\pm, \\
\mu_\pm =& \sum_{i_1} \frac{\eta_{i_1}^2}{\Omega - \omega_{a_{i_1}} + i(\pm\frac{\Gamma}{2} + \varepsilon)} \\
&+ \sum_{n=2}^{\infty} \sum_{i_1} \sum_{i_2, i_2 \neq i_1} \cdots \sum_{i_n, i_n \neq i_{n-1}} \frac{\eta_{i_1}\beta_{i_1 i_2}\cdots\beta_{i_{n-1} i_n}\eta_{i_n}}{\prod_{l=1}^{n}[\Omega - \omega_{a_{i_l}} + i(\pm\frac{\Gamma}{2} + \varepsilon)]}.
\end{aligned}
\tag{28}
$$

We note that a self-consistent solution must satisfy the continuous boundary condition $e(0^+) = e(0^-)$. However, it can be directly checked that $e(0^+) \neq e(0^-)$ due to the $\mu_\pm$ terms from coupling to the reservoir, indicating that $|B_K\rangle$ is not an eigenstate.

Reservoir-modified two-photon bound state: To find the reservoir-modified two-photon bound state solution, we start with the following general form in Region 3 ($x_1 < x_2 < 0$):

$$
\phi(x_1, x_2) = e^{i\frac{\omega_{k_1}}{v_g}x_1 + i\frac{\omega_{k_2}}{v_g}x_2}, \tag{29}
$$

where ω_{k_1} and ω_{k_2} are angular frequencies of two respective photons that are to be determined from boundary conditions. In general, ω_{k_1} and ω_{k_2} are complex numbers. We now adopt the

aforementioned *divide and conquer* scheme, and obtain the interacting eigen wavefunctions of H_e for the restricted state variables (*i.e.*, $\phi(x_1, x_2)$ and $e(x)$), as shown in Fig. 6, where

$$\begin{aligned}\Omega_{1,2} =&\Omega + \mu_{1,2},\\ \mu_{1,2} =&\sum_{i_1} \frac{\eta_{i_1}^2}{\omega_{k_{1,2}} - \omega_{a_{i_1}} + i\varepsilon}\\ &+\sum_{n=2}^{\infty}\sum_{i_1}\sum_{i_2,i_2\neq i_1}\cdots\sum_{i_n,i_n\neq i_{n-1}} \frac{\eta_{i_1}\beta_{i_1 i_2}\cdots\beta_{i_{n-1}i_n}\eta_{i_n}}{\prod_{l=1}^{n}(\omega_{k_{1,2}} - \omega_{a_{i_l}} + i\varepsilon)}.\end{aligned} \tag{30}$$

And the transmission coefficient for the reservoir-modified two-photon bound state $\widetilde{t}_K^{(2)}$ is given by

$$\widetilde{t}_K^{(2)} = \frac{\omega_{k_1} - \Omega_1 - i\Gamma/2}{\omega_{k_2} - \Omega_2 + i\Gamma/2}. \tag{31}$$

To determine the photon frequencies, we now impose the boundary condition $e(0^+) = e(0^-)$, and the energy conservation condition $\omega_{k_1} + \omega_{k_2} = Kv_g$, thus leading to

$$\begin{aligned}\omega_{k_1} &= \frac{Kv_g}{2} - \frac{\mu_2 - \mu_1}{2} - i\frac{\Gamma}{2},\\ \omega_{k_2} &= \frac{Kv_g}{2} + \frac{\mu_2 - \mu_1}{2} + i\frac{\Gamma}{2}.\end{aligned} \tag{32}$$

Further simplification arrives by imposing the following two constraints: (1) the summation of ω_{k_1} and ω_{k_2} is a real number, Kv_g, indicating ω_{k_1} and ω_{k_2} are complex conjugate numbers; (2) for the atomic excitation amplitude $e(x)$, as given in Fig. 6, to remain finite for all x, we must have $\mathrm{Im}(\omega_{k_1}) < 0$ and $\mathrm{Im}(\omega_{k_2}) > 0$ (Im represents the imaginary part of a complex number). Thus, the photon frequencies should take the following form

$$\begin{aligned}\omega_{k_1} &= \xi_1\frac{Kv_g}{2} - i\frac{\Gamma}{2}\nu,\\ \omega_{k_2} &= \xi_2\frac{Kv_g}{2} + i\frac{\Gamma}{2}\nu,\end{aligned} \tag{33}$$

where $\xi_{1,2} = 1 \mp \mathrm{Re}(\mu_2 - \mu_1)/Kv_g$ and $\nu = 1 + \mathrm{Im}(\mu_2 - \mu_1)/\Gamma$. Note that $\nu > 0$ is required for Eq. (32) to have solutions. By plugging Eq. (33) into Eq. (29), Eq. (29) now reads as $e^{iK\widetilde{x}_c + \kappa\nu(x_1 - x_2)/2}$, where $\widetilde{x}_c = (\xi_1 x_1 + \xi_2 x_2)/2$ is the position of the center of mass of two photons when the reservoir is present.

Noting that in the reservoir-free case, the transmission coefficient for the bound state is $t_K^{(2)} = (Kv_g/2 - \Omega - i\Gamma)/(Kv_g/2 - \Omega + i\Gamma)$. We can show that $\widetilde{t}_K^{(2)}$ reduces to $t_K^{(2)}$ in the absence of the reservoir. Specifically, in the absence of the reservoir (*i.e.*, $\eta = \beta = 0$), $\omega_{k_1} = Kv_g/2 - i\Gamma/2$, $\omega_{k_2} = Kv_g/2 + i\Gamma/2$, and $\Omega_{1,2} = \Omega$. By plugging such relations into

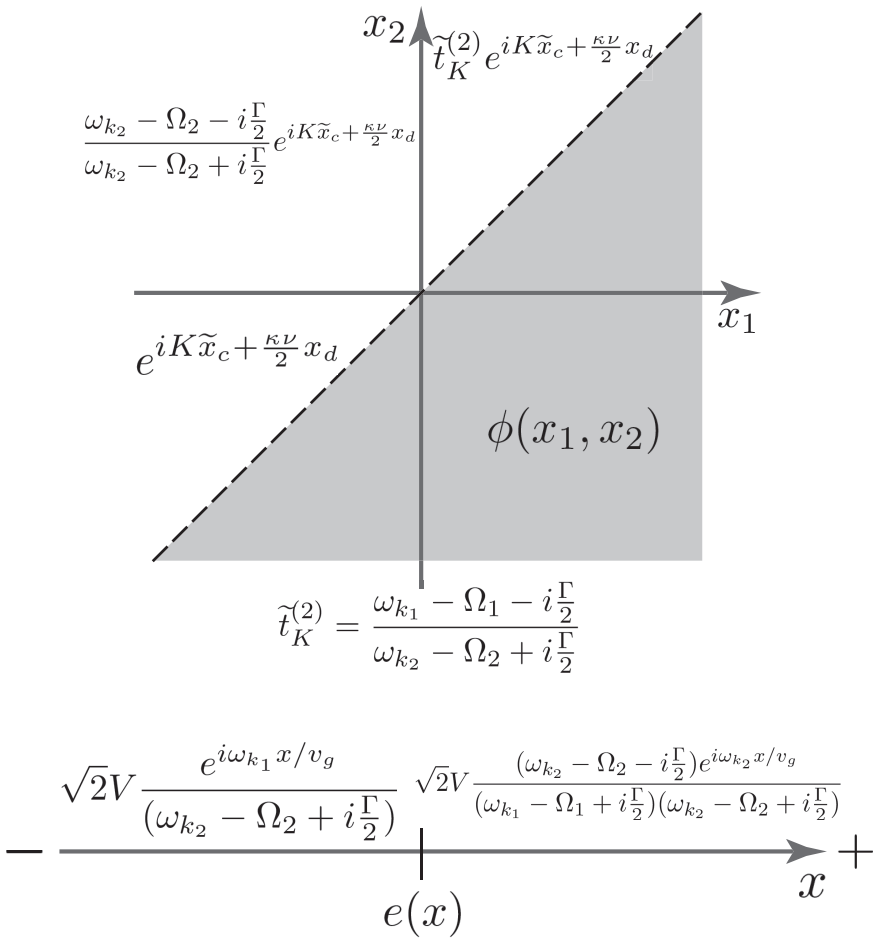

FIG. 6. Interacting eigenstate solution of the restricted system variables $\phi(x_1, x_2)$ and $e(x)$ to Eqs. (13) for the reservoir-modified two-photon bound state case.

Eq. (31), $\widetilde{t}_K^{(2)}$ reduces to $t_K^{(2)}$. Nonetheless, when the reservoir is present, the renormalized transmission coefficient for the reservoir-modified bound state $\widetilde{t}_K^{(2)}$ can not be obtained by simply using a frequency renormalization in $t_K^{(2)}$.

We now construct the normalized reservoir-modified bound state $|D_K\rangle$ based on the restricted system variables of the interacting eigenstate (shown in Fig. 6), which takes the following form,

$$
\begin{aligned}
|D_K\rangle &= \iint dx_1 dx_2 D_K(x_1,x_2)\frac{1}{\sqrt{2}}c_e^\dagger(x_1)c_e^\dagger(x_2), \quad \text{where} \\
D_K(x_1,x_2) &= \sqrt{\frac{\kappa\nu}{4\pi}}e^{iK\frac{\xi_1 x_1+\xi_2 x_2}{2}-\frac{\kappa\nu}{2}|x_1-x_2|}.
\end{aligned}
\tag{34}
$$

By applying the Fourier transform on $D_K(x_1, x_2)$ from real space to momentum space (*i.e.*, $D_K(k_1,k_2) = \iint dk_1 dk_2 D_K(x_1,x_2)e^{-i(k_1x_1+k_2x_2)}/2\pi$), one obtains that $D_K(k_1,k_2) =$

$\sqrt{\kappa^3\nu^3/4\pi}\delta(K-k_1-k_2)/[(k_1-\xi_1 K/2)^2+\kappa^2\nu^2/4]$. The Dirac-$\delta$ function here (*i.e.*, $\delta(K-k_1-k_2)$) again indicates that the two photons described by the reservoir-modified bound state is anti-correlated in the momentum space.

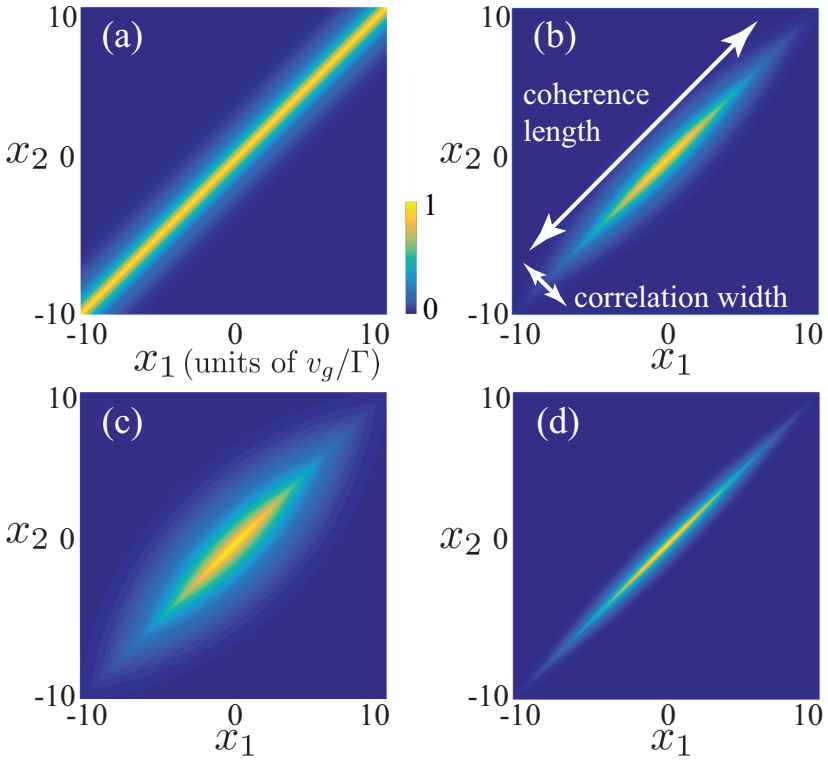

FIG. 7. Wave function density plot for the reservoir-free two-photon bound state $|B_K\rangle$ and the reservoir-modified two-photon bound state $|D_K\rangle$. (a) Two-photon bound state $|B_K|^2$. (b) Gaussian-modulated two-photon bound state $|B_K\mathcal{M}|^2$. The correlation length and the coherence width are given by $1/\kappa$ and σ_x, respectively. $|B_K\mathcal{M}|^2$ is centered at $x_1 = x_2 = x_o = 0$. (c) Gaussian-modulated reservoir-modified bound state $|D_K\mathcal{M}|^2$ when $\nu = 0.5$. (d) $|D_K\mathcal{M}|^2$ when $\nu = 2$. For the density plot, the numerical values of one unit scale is (a) 0.4, (b) 0.0025, (c) 0.00012, and (d) 0.005 in units of Γ^2/v_g^2 (which has a unit of 1/Length^2).

To illustrate the reservoir-induced effect on the bound state, we now plot the wave function density for the bound state $|B_K\rangle$ and the reservoir-modified bound state $|D_K\rangle$ in Fig. 7. Figure 7(a) plots $|B_K|^2$ wherein the bound state is unmodulated and thus extends along the diagonal ($x_1 = x_2$); the state has a correlation width of $1/\kappa$ along the transverse direction ($x_1 = -x_2$). That is, two photons propagate in a collocated manner within a spatial range of $1/\kappa$. To represent a practical pulse of finite spatial size, we plot the density for a Gaussian-

modulated bound state $|B_K\mathcal{M}|^2$ in Fig. 7(b) using the same parameter set of $\mathcal{M}$ as the preceding plane-wave case. For the modulated state, the spatial size of the modulation is the coherence length, which also determines the coherence time of the pulse. Specifically, the coherence length of $|B_K\mathcal{M}|^2$ is determined by the Gaussian modulation parameter σ_x while the correlation width remains the same as $|B_K|^2$. We further plot the wave function density of the Gaussian-modulated reservoir-modified bound state $|D_K\mathcal{M}|^2$ to visualize the effect of the reservoir on the bound state. Figure 7(c) and (d) plot $|D_K\mathcal{M}|^2$ for $\nu = 0.5$ and $\nu = 2$, respectively, wherein the correlation width is doubled and halved, respectively. That is, the correlation width of $|D_K\mathcal{M}|^2$ now becomes $1/\kappa\nu$ where varying ν values depends on the system-reservoir coupling (*i.e.*, described by η) and the secondary scattering strength in the reservoir (*i.e.*, described by β). Unmodulated reservoir-modified bound state $|D_K|^2$ is not plotted because all entanglement information is already provided in the plots for the modulated case in Fig. 7(c) and (d).

D. Restricted scattering matrix

The information of the scattering eigenstates of the system dictates the scattering matrix. The scattering matrix $\mathbf{S}$ maps an arbitrary in-state (the prepared photonic state injected into the waveguide) into the out-state: $\mathbf{S}|\text{in}\rangle = |\text{out}\rangle$ [26]. In reality, however, only the waveguided photonic states are measurable but not those leaked into the reservoir. Consequently, a *restricted* scattering matrix which maps the in-state into the waveguided photonic states solely is of practical importance. In this section, we discuss the construction of the restricted scattering matrix for the excitable-reservoir case.

Due to the presence of the reservoir, to which the photons leak into, the waveguided out-states are spanned by the set of bases consisting of zero-photon (both photons leak to the reservoir), one-photon (one photon leaks to the reservoir), and two-photon Fock states. As a comprehensive treatment of the complete restricted scattering matrix is rather involved, here we will limit the discussion to the two-photon sector of the the restricted scattering matrix $\mathbf{S}^r_{e^{(2)}}$ for the even-mode case which is described by Eq. (11). (That is, the output waveguided photonic states contain two photons.) The generalization to include the zero- and one-photon sectors are straightforward.

By construction, $|D_K\rangle$ is a scattering eigenstate of the restricted scattering matrix

$\mathbf{S}^r_{e^{(2)}}$ such that $\mathbf{S}^r_{e^{(2)}}|D_K\rangle = \widetilde{t}^{(2)}_K|D_K\rangle$. One can directly check the orthogonality relation $\langle D_{K'}|D_K\rangle = \delta(K-K')2\sqrt{\nu\nu'}/(\nu+\nu')$, where ν and ν' are determined by K and K', respectively. In Ref. [26], it has been confirmed that the reservoir-free two-photon bound state $|B_K\rangle$ is orthogonal to the two-photon plane-wave state $|W_{k,p}\rangle$, *i.e.,* $\langle W_{k,p}|B_K\rangle = 0\ \forall k$, p, and K. In contrast, when the excitable reservoir is present, we find that

$$\langle W_{k,p}|D_K\rangle = \sqrt{\frac{\kappa^3\nu}{2\pi}}\frac{(\nu-1)\Delta}{\sqrt{\Delta^2+\frac{\kappa^2}{4}}\left(\Delta^2+\frac{\kappa^2\nu^2}{4}\right)}\delta(K-(k+p)). \tag{35}$$

(Note that $|W_{k,p}\rangle$ has the same form for both the reservoir-free case and the excitable-reservoir case, as described above.) That is, the reservoir-modified bound state $|D_K\rangle$ and the plane-wave state $|W_{k,p}\rangle$ are degenerate and *not* orthogonal when the two states have the same energy *i.e.,* $\langle W_{k,p}|D_K\rangle \neq 0$ when $K = k+p$. The fact that the two states have a non-zero overlap at the same energy indicates the two states can transform to each other. The physical reason is that, due to the existence of the scatterers in the excitable reservoir, when a waveguided photon in either state leaks into the reservoir, the photon has a non-zero amplitude to scatter back to the waveguide. The re-entrant photon can form a different state with the remaining photon.

Thus, the restricted out-state of an arbitrary in-state can be straightforwardly obtained by decomposing the in-state into linear superposition of $|W_{k,p}\rangle$ and $|D_K\rangle$, and followed by operating the scattering matrix on each eigenstate. To this end, we investigate the explicit form of $\mathbf{S}^r_{e^{(2)}}$ under the bases of its eigenstates, $|W_{k,p}\rangle$ and $|D_K\rangle$, which, by imposing eigen-relations $\mathbf{S}^r_{e^{(2)}}|W_{k,p}\rangle = \bar{t}_k\bar{t}_p|W_{k,p}\rangle$ and $\mathbf{S}^r_{e^{(2)}}|D_K\rangle = \widetilde{t}^{(2)}_K|D_K\rangle$, after some algebra, can be shown to have the following form

$$\begin{aligned}
\mathbf{S}^r_{e^{(2)}} =& \sum_{k\leq p}\bar{t}_k\bar{t}_p|W_{k,p}\rangle\langle W_{k,p}| + \sum_K \widetilde{t}^{(2)}_K\frac{(1+\nu)^2}{4\nu}|D_K\rangle\langle D_K| \\
&- \sum_{k\leq p,K}\bar{t}_k\bar{t}_p\sqrt{\frac{\kappa^3\nu}{2\pi}}\frac{(\nu-1)\Delta}{\sqrt{\Delta^2+\frac{\kappa^2}{4}}\left(\Delta^2+\frac{\kappa^2\nu^2}{4}\right)}\frac{(1+\nu)^2}{4\nu}\delta(K-k-p)|W_{k,p}\rangle\langle D_K| \\
&- \sum_{k\leq p,K}\widetilde{t}^{(2)}_K\sqrt{\frac{\kappa^3\nu}{2\pi}}\frac{(\nu-1)\Delta}{\sqrt{\Delta^2+\frac{\kappa^2}{4}}\left(\Delta^2+\frac{\kappa^2\nu^2}{4}\right)}\frac{(1+\nu)^2}{4\nu}\delta(K-k-p)|D_K\rangle\langle W_{k,p}| \\
&+ \sum_{k_1\leq p_1,k_2\leq p_2}\bar{t}_{k_1}\bar{t}_{p_1}\sum_K\frac{\kappa^3\nu}{2\pi}\frac{(\nu-1)^2\Delta_1\Delta_2}{\sqrt{\left(\Delta_1^2+\frac{\kappa^2}{4}\right)\left(\Delta_2^2+\frac{\kappa^2}{4}\right)\left(\Delta_1^2+\frac{\kappa^2\nu^2}{4}\right)\left(\Delta_2^2+\frac{\kappa^2\nu^2}{4}\right)}}\frac{(1+\nu)^2}{4\nu} \\
&\times\delta(K-k_1-p_1)\delta(K-k_2-p_2)|W_{k_1,p_1}\rangle\langle W_{k_2,p_2}|,
\end{aligned} \tag{36}$$

where $\Delta_{1,2} = (k_{1,2} - p_{1,2})/2$. Here, we note that the off-diagonal terms emerge because the scattering eigenstates are non-orthogonal.

To compare the results in the excitable reservoir scenario here with those in the reservoir-free and non-excitable scenarios to gain deeper insights, we now express the scattering matrix in terms of orthogonal bases $|W_{k,p}\rangle$ and $|B_K\rangle$. In the reservoir-free case, $|W_{k,p}\rangle$ and $|B_K\rangle$ are orthogonal eigenstates of the scattering matrix so that the scattering matrix is diagonal, given by $\mathbf{S}_{e^{(2)}} = \sum_{k\leq p} t_k t_p |W_{k,p}\rangle\langle W_{k,p}| + \sum_K t_K |B_K\rangle\langle B_K|$ [24]; and in the non-excitable reservoir scenario, *e.g.*, a surrounding vacuum or homogeneous dielectric medium, to which the waveguided photons leak into, the restricted scattering matrix is $\mathbf{S}^r_{e^{(2)}} = \sum_{k\leq p} \bar{t}'_k \bar{t}'_p |W_{k,p}\rangle\langle W_{k,p}| + \sum_K \bar{t}'^{(2)}_K |B_K\rangle\langle B_K|$, where $\bar{t}'_{k,p} = (\omega_{k,p} - \bar{\Omega}' - i\Gamma/2)/(\omega_{k,p} - \bar{\Omega}' + i\Gamma/2)$, $\bar{t}'^{(2)}_K = (Kv_g - 2\bar{\Omega}' - 2i\Gamma)/(Kv_g - 2\bar{\Omega}' + 2i\Gamma)$, and the renormalized frequency $\bar{\Omega}' = \Omega - i\gamma_S$, where γ_S is the photonic scattering loss rate [8]. Here, for the excitable reservoir case, Eq. (36) can be recast into the following form

$$\begin{aligned}\mathbf{S}^r_{e^{(2)}} =& \sum_{k\leq p} \bar{t}_k \bar{t}_p |W_{k,p}\rangle\langle W_{k,p}| + \sum_K \widetilde{\bar{t}}^{(2)}_K |B_K\rangle\langle B_K| \\ &+ \sum_{k\leq p}\sum_K \sqrt{\frac{\kappa^3}{8\pi}} \frac{(\nu^2-1)\Delta}{\sqrt{\Delta^2 + \frac{\kappa^2}{4}}\left(\Delta^2 + \frac{\kappa^2\nu^2}{4}\right)} (\widetilde{\bar{t}}^{(2)}_K - \bar{t}_k \bar{t}_p)\delta(K-k-p)|W_{k,p}\rangle\langle B_K|,\end{aligned} \tag{37}$$

where the first term describes the transmission of uncorrelated two-photon states, while second and third terms describe the transmission of correlated states. We note that the off-diagonal term that maps the correlated state $|B_K\rangle$ to uncorrelated state $|W_{k,p}\rangle$.

Furthermore, it can be straightforwardly shown that $\mathbf{S}^r_{e^{(2)}} \mathbf{S}^{r\,\dagger}_{e^{(2)}} \neq 1$, indicating that $\mathbf{S}^r_{e^{(2)}}$ is not unitary. When the external reservoir is present, the resulting photon loss leads to a non-unitary property as the total photonic flux in the waveguide is not conserved and decreased (i.e., transmission coefficients, $|\bar{t}'_k \bar{t}'_p|^2$, $|\bar{t}_k \bar{t}_p|^2$, $|\bar{t}'^{(2)}_K|^2$, and $|\widetilde{\bar{t}}^{(2)}_K|^2 < 1$). The properties of the restricted scattering matrix for each scenario are summarized in Table I.

Finally, we comment on the validity of the reduced Hamiltonian approach for the two-photon transport. For the plane-wave state solution, the functional form of the interacting eigenstate for the restricted system variables (*i.e.*, $\phi(x_1, x_2)$, $e(x)$), and transmission coefficients follow similar forms to those in the reservoir-free case, with a frequency renormalization ($\Omega \to \bar{\Omega}$). For the reservoir-modified bound state solution, however, the functional form of the interacting states for restricted system variables and $\widetilde{\bar{t}}^{(2)}_K$ cannot be easily obtained from those in the reservoir-free case simply by a frequency renormalization. Consequently,

TABLE I. Properties of restricted scattering matrix $\mathbf{S}^r_{e^{(2)}}$ in the $\{|W_{k,p}\rangle, |B_K\rangle\}$ bases.

Scenarios	Diagonal	Unitary
reservoir-free[a]	$\surd$	$\surd$
non-excitable	$\surd$	$\times$
excitable	$\times$	$\times$

[a] Refer to the scattering matrix $\mathbf{S}_{e^{(2)}}$.

due to the existence of the bound states, the effect of the reservoir in general can not be described by a reduced Hamiltonian approach.

E. Weak-reservoir Condition

For scenarios wherein the material loss is weak (but the photonic scattering loss can be arbitrary as the reduced Hamiltonian approach is valid for arbitrary photonic scattering loss [8]), we derive the condition such that the reduced Hamiltonian approach is approximately valid for the two-photon case. This is called the weak-reservoir condition.

The weak-reservoir condition requires: the system-reservoir coupling $\bar{\eta}$ and the secondary scattering strength $\bar{\beta}$ are both weak enough, *i.e.*, $\bar{\eta}, \bar{\beta} \ll \Omega, \Gamma$; and the photon-reservoir detuning $\bar{\delta}$ is much larger than the photon-atom interaction strength, *i.e.*, $\bar{\delta} \gg \Gamma/2$. When such a condition is fulfilled, the photon frequencies of the reservoir-modified bound state are approximated by $\omega_{k_1} \approx \Omega - i\Gamma/2$ and $\omega_{k_2} \approx \Omega + i\Gamma/2$ because $\|\mu_{1,2}\| \approx \frac{\bar{\eta}^2 \bar{D}\Delta\omega/\bar{\delta}}{1-\bar{\beta}\bar{D}\Delta\omega/\bar{\delta}} \ll \Omega, \Gamma$ and $\|\mu_1 - \mu_2\|/2 \ll \Omega, \Gamma$ (where $\|\|$ denotes the norm of a complex number and we have used the relation $\bar{D}\Delta\omega \approx 1$, $\bar{\beta}/\bar{\delta} \ll 1$, $\bar{\eta}/\bar{\delta} \ll 1$, and $\bar{\eta} \ll \Omega, \Gamma$). Noting that $\Omega - \omega_{a_j} + i(\pm\Gamma/2 + \varepsilon) \approx \Omega - \omega_{a_j} + i\varepsilon$ due to larger photon-reservoir detuning. One now plugs such approximations into $\mu_{1,2}$ (Eq. (30)) to obtain $\mu_1 \approx \mu_2 \approx \alpha$, and $\Omega_1 \approx \Omega_2 \approx \bar{\Omega}$. It is worth noting that when both criteria are satisfied, $\bar{\beta} \ll \Gamma \ll \bar{\delta}$, and $\bar{D}\Delta\omega \approx 1$. That is, $\bar{\beta}\bar{D}\Delta\omega/\bar{\delta} \ll 1$ is fulfilled such that α can be approximated by its first-order term (*i.e.*, $\alpha \approx \alpha_1$). When the weak-reservoir condition is satisfied, the interacting eigenstates for the restricted system variables for the reservoir-modified bound state solution (shown in Fig. 6) reduces to the functional forms in Fig. 8. As can be immediately identified, $\phi(x_1, x_2)$ and $e(x)$ now follow similar functional forms to those in the reservoir-free case that can be described by a frequency renormalization

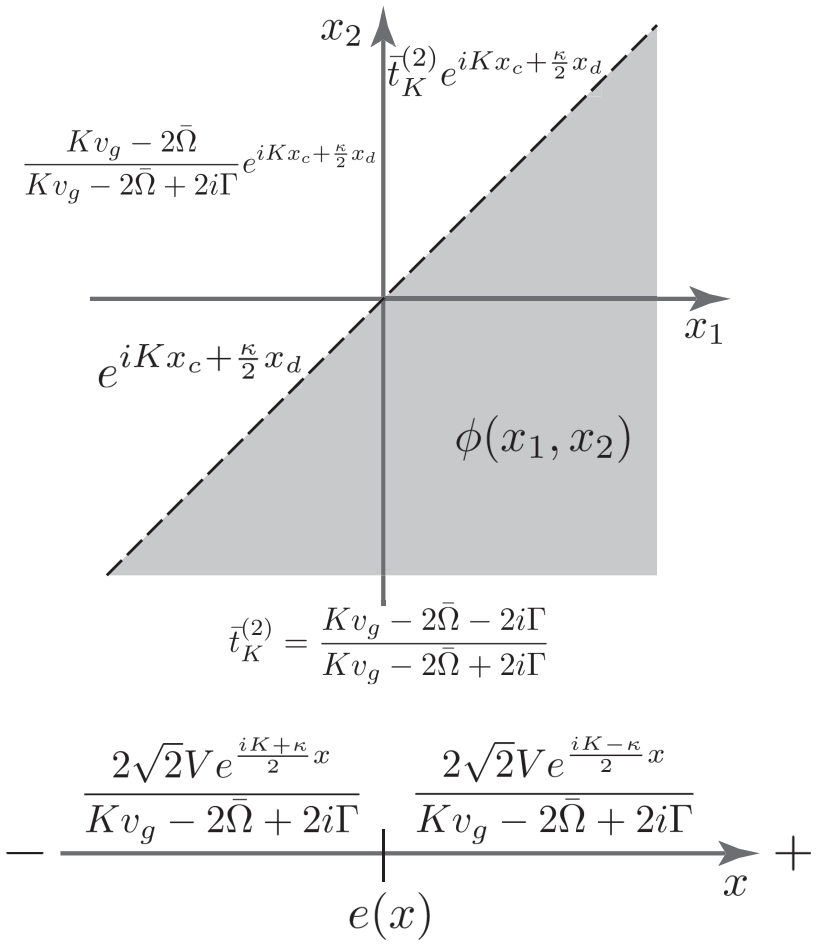

FIG. 8. Interacting eigenstate solution of the restricted system variables $\phi(x_1, x_2)$ and $e(x)$ to Eqs. (13) for the reservoir-modified two-photon bound state case when the weak-reservoir condition is satisfied.

$\Omega \to \bar{\Omega} = \Omega + \Delta - i\gamma$. Thus, the solutions for both the plane-wave state (Fig. 4) and the bound state (Fig. 8) are renormalized by a frequency renormalization ($\Omega \to \bar{\Omega}$). As a result, the reduced Hamiltonian approach remains valid for the two-photon case when the weak-reservoir condition is satisfied. The same conclusions apply to the two-photon two-mode case.

V. N-PHOTON CASE

Having studied the single-photon and the two-photon cases, we now examine the case for an arbitrary N-photon Fock state transport. It has been rigorously confirmed that, in the reservoir-free case, a complete set of N-photon in-states can be classified into three

categories, *i.e.*, the N-photon extended state, N-photon bound state, and N-photon hybrid states [25]. Specifically, the N-photon extended state is a generalization of two-photon plane-wave state to the N-photon case, wherein all N photons are uncorrelated. For the N-photon bound state, all photons are entangled. In particular, any two-photon pair is spatially characterized by a correlation width v_g/Γ. The N-photon hybrid states are product states of plane-wave and bound states. Hereafter we will focus on the extended and bound state solutions. The hybrid state case can be examined through a similar procedure.

A. General State and Equations of Motion

To describe the N-photon scattering process, the N-photon interacting eigenstate describing the combined system in the even mode, $|\Phi_N\rangle$ is given by

$$\begin{aligned}|\Phi_N\rangle =&\Big(\int\cdots\int\prod_{l=1}^{N}dx_l\phi(x_1,\cdots,x_N)\frac{\prod_{m=1}^{N}c_e^\dagger(x_m)}{\sqrt{N!}}\\&+\int\cdots\int\prod_{l=1}^{N-1}dx_l e(x_1,\cdots,x_{N-1})\frac{\sigma_+\prod_{m=1}^{N-1}c_e^\dagger(x_m)}{\sqrt{(N-1)!}}\\&+\sum_j\int\cdots\int\prod_{l=1}^{N-1}dx_l\phi_j(x_1,\cdots,x_{N-1})\frac{\sigma_{j+}\prod_{m=1}^{N-1}c_e^\dagger(x_m)}{\sqrt{(N-1)!}}\\&+\sum_j\int\cdots\int\prod_{l=1}^{N-2}dx_l e_j(x_1,\cdots,x_{N-2})\frac{\sigma_+\sigma_{j+}\prod_{m=1}^{N-2}c_e^\dagger(x_m)}{\sqrt{(N-2)!}}\\&+\cdots\Big)|\varnothing\rangle,\end{aligned}\tag{38}$$

where only variables that are relevant to our analysis are explicitly given above. $\phi(x_1,\cdots,x_N)$ denotes the wave function for N waveguided photons. $e(x_1,\cdots,x_{N-1})$ is the atomic excitation amplitude wherein one photon is absorbed by the atom, and the other $N-1$ photons remain waveguided. $\phi_j(x_1,\cdots,x_{N-1})$ is the oscillator excitation amplitude wherein one photon is absorbed by the j-th oscillator while the other $N-1$ photons remain waveguided. $e_j(x_1,\cdots,x_{N-2})$ represents the excitation amplitude wherein two photons are absorbed by the atom and the j-th oscillator, respectively, and the other $N-2$ photons are waveguided. By applying Schrödinger Equation $H_e|\Phi_N\rangle=\hbar\tilde{\epsilon}|\Phi_N\rangle$, one obtains the following equations

of motion that are relevant to our analysis,

$$\begin{aligned}
&\epsilon\phi(x_1,\ldots,x_N) = (-iv_g\sum_{l=1}^{N}\partial x_l)\phi(x_1,\ldots,x_N)\\
&+\frac{V}{\sqrt{N}}\sum_{l=1}^{N}\delta(x_l)e(x_1,\cdots,x_{l-1},x_{l+1},\cdots,x_N),
\end{aligned} \tag{39a}$$

$$\begin{aligned}
&\epsilon e(x_1,\ldots,x_{N-1}) = (-iv_g\sum_{l=1}^{N-1}\partial x_l)e(x_1,\ldots,x_{N-1})\\
&+\frac{V}{\sqrt{N}}\left[\phi(0,x_1,\ldots,x_{N-1})+\cdots+\phi(x_1,\ldots,x_{N-1},0)\right]\\
&+\Omega e(x_1,\ldots,x_{N-1})+\sum_j\eta_j\phi_j(x_1,\ldots,x_{N-1}),
\end{aligned} \tag{39b}$$

$$\begin{aligned}
&\epsilon\phi_j(x_1,\ldots,x_{N-1}) = (-iv_g\sum_{l=1}^{N-1}\partial x_l)\phi_j(x_1,\ldots,x_{N-1})\\
&+\frac{V}{\sqrt{N-1}}\sum_{l=1}^{N-1}\delta(x_l)e_l(x_1,\cdots,x_{l-1},x_{l+1},\cdots,x_{N-1})\\
&+\omega_{a_j}\phi_j(x_1,\ldots,x_{N-1})+\eta_j e(x_1,\ldots,x_{N-1}),
\end{aligned} \tag{39c}$$

where $\hbar\tilde{\epsilon} = \hbar(\epsilon+\omega_g+\sum_j\omega_{g_j})$ is the total energy of the combined system with $\hbar\epsilon$ being the energy of incident N photons. Due to bosonic symmetry and wave function continuity at the boundary, only the restricted region of $x_1 < x_2 < \cdots < x_N$ is considered. To facilitate the description of the *divide and conquer* scheme, we now further divide such a region into $N+1$ ordered sub-regions, which are specified by

$$\begin{cases}
x_1 < x_2 < \cdots < x_N < 0, & \text{Region } N+1\\
x_1 < x_2 < \cdots < x_{j-1} < 0 < x_j < \cdots < x_N, & \text{Region } j, \quad j = N, N-1, \cdots, 2\\
0 < x_1 < x_2 < \cdots < x_N, & \text{Region 1.}
\end{cases} \tag{40}$$

Region $N+1$ and Region 1 correspond to the cases before and after scattering, respectively while all other regions correspond to the cases during the scattering process.

Here we introduce our computational strategy. We first solve Eqs. (39) to obtain the solution of the interacting eigenstates of H_e for restricted system variables (*i.e.*, ϕ and e). In particular, we will show that the reservoir degrees of freedom (*i.e.*, ϕ_j, e_j, and those that are omitted in Eq. (38)) can be traced over and are not relevant to our analysis. By applying the *divide and conquer* scheme, the interacting eigenstates are solved for to obtain in- and out-states, which are further normalized to construct the eigenstates of the restricted S-matrix.

B. N-photon Extended State Solution When The Reservoir Is Present

Following the Bethe Ansatz in the N-particle case, the wave function for the N-photon extended state in Region $N+1$ takes the following form,

$$\phi(x_1,\cdots,x_N)=\sum_{\mathcal{P}\in S_N}\mathcal{A}_{N+1}(\mathcal{P})\exp\Big(i\sum_{j=1}^{N}\frac{\omega_{k_j}}{v_g}x_{\mathcal{P}_j}\Big), \tag{41}$$

where $\omega_{k_1},\cdots,\omega_{k_N}$ are real-valued angular frequencies of N respective photons subject to the energy conservation constraint $\sum_{j=1}^{N}\omega_{k_j}=\epsilon$. S_N is the permutation group of the set $\{1,2,\cdots,N\}$. $\mathcal{P}$ is an element of S_N specifying one particular permutation. $\mathcal{P}_j$ denotes the j-th location in a specific arrangement $\mathcal{P}$. $\mathcal{A}_{N+1}$ denotes the coefficient in Region $N+1$. Following the *divide and conquer* scheme (Region $N+1\rightarrow N\rightarrow\cdots\rightarrow 1$), one obtains the following transmitted wave function in Region 1,

$$\phi(x_1,\cdots,x_N)=\prod_{j=1}^{N}\bar{t}_{k_j}\sum_{\mathcal{P}\in S_N}\mathcal{A}_{N+1}(\mathcal{P})\exp\Big(i\sum_{m=1}^{N}\frac{\omega_{k_m}}{v_g}x_{\mathcal{P}_m}\Big), \tag{42}$$

where $\bar{t}_{k_j}=(\omega_{k_j}-\bar{\Omega}-i\Gamma/2)/(\omega_{k_j}-\bar{\Omega}+i\Gamma/2)$ is the aforementioned renormalized single-photon transmission coefficient in the even mode. The atomic excitation wave function e can be determined, which follows a similar functional form to that in the reservoir-free case but with a frequency renormalization $\Omega\rightarrow\bar{\Omega}$. Based on the interacting eigenstate for the restricted system variables (*i.e.*, $|\Phi_N\rangle=\Big[\int\cdots\int\prod_{l=1}^{N}dx_l\phi(x_1,\cdots,x_N)\prod_{m=1}^{N}c_e^{\dagger}(x_m)/\sqrt{N!}+\int\cdots\int\prod_{l=1}^{N-1}dx_l e(x_1,\cdots,x_{N-1})\sigma_+\prod_{m=1}^{N-1}c_e^{\dagger}(x_m)/\sqrt{(N-1)!}\Big]|\varnothing\rangle$), we can construct the following normalized N-photon extended state as an eigenstate of the restricted S-matrix $\mathbf{S}^r_{e^{(N)}}$ in the N-photon Hilbert space,

$$\begin{aligned}|W_{k_1,\cdots,k_n}\rangle=&\int\cdots\int\prod_{l=1}^{N}dx_l\frac{v_g^{\frac{N(N-1)}{2}}}{\sqrt{\prod_{m<n}[\omega_{k_m}^2-\omega_{k_n}^2]+\Gamma^2)N!(2\pi)^N}}\\&\sum_{\mathcal{P}\in S_N}\mathcal{A}_{N+1}(\mathcal{P})\exp\Big(i\sum_{j=1}^{N}\frac{\omega_{k_j}}{v_g}x_{\mathcal{P}_j}\Big)\frac{\prod_{m=1}^{N}c_e^{\dagger}(x_m)}{\sqrt{N!}},\end{aligned} \tag{43}$$

such that $\mathbf{S}^r_{e^{(N)}}|W_{k_1,\cdots,k_n}\rangle=\prod_{j=1}^{N}\bar{t}_{k_j}|W_{k_1,\cdots,k_n}\rangle$. We note that the N-photon extended state remains the same form as that in the reservoir-free case whereas the transmission amplitudes are renormalized. The aforementioned single-photon and the two-photon plane-wave cases are special cases. The form of the extended state solution indicates that the N photons interact with the lossy atom independently.

C. N-photon Bound State Solution When The Reservoir Is Present

Reservoir-free case: To describe the N-photon scattering processes, we also need to find the complete set of $\mathbf{S}^r_{e^{(N)}}$ that spans the N-photon Hilbert space. Such a complete set has been analytically investigated in Ref. [25]. Among all admissible N-photon states, a particular entangled state of interest is the N-photon bound state, *i.e.*, $|B_K\rangle = \int\cdots\int\prod_{l=1}^N dx_l B_K(x_1,\cdots,x_N)\frac{\prod_{m=1}^N c_e^\dagger(x_m)}{\sqrt{N!}}$, where $B_K(x_1,\cdots,x_N) = \sqrt{\frac{\kappa^{N-1}(N-1)!}{2N\pi}}e^{iKx_c-\frac{\kappa\sum_{m<n}|x_m-x_n|}{2}}$. $x_c = \sum_{j=1}^N x_j/N$ and $K = \epsilon/v_g$ are the center position and total wave vector of N photons, respectively. In the reservoir-free case, given the total energy $\hbar K v_g$ of N photons, the frequencies of the N-photon bound state is given by $\omega_{k_1} = Kv_g/N - i(N-1)\Gamma/2, \omega_{k_2} = Kv_g/N - i(N-3)\Gamma/2,\cdots,\omega_{k_N} = Kv_g/N + i(N-1)\Gamma/2$. The probability amplitude decays exponentially as the distance between any two photons increases. In the momentum space representation, it can be shown that the momentum wave function $B_K(k_1,\cdots,k_N) \equiv \int\cdots\int\prod_{l=1}^N x_l B_K(x_1,\cdots,x_N)e^{-i\sum_{m=1}^N k_m x_m}/(2\pi)^{N/2}$ yields $B_K(k_1,\cdots,k_N)\propto\delta(K-\sum_{l=1}^N k_l)$, indicating that the frequencies of the N photons in the N-photon bound state are anti-correlated.

Reservoir is present: Similar to the two-photon case, it can be shown that the N-photon bound state $|B_K\rangle$ fails to be an eigenstate of restricted scattering matrix $\mathbf{S}^r_{e^{(N)}}$ in the presence of the reservoir, as it would give rise to a discontinuity of the atomic excitation wave function (*i.e.*, $e(x_1,\cdots,x_{N-1})$ is not continuous at the boundary between any two adjacent Region $j+1$ and j for $j=1,\cdots,N$).

Reservoir-modified N-photon bound state: To find the reservoir-modified N-photon bound state solution, we start with the following general form in Region $N+1$,

$$\phi(x_1,\cdots,x_N) = \exp\left[i\left(\frac{\omega_{k_1}}{v_g}x_1 + \frac{\omega_{k_2}}{v_g}x_2 + \cdots\frac{\omega_{k_N}}{v_g}x_N\right)\right], \tag{44}$$

where $\omega_{k_1},\cdots,\omega_{k_N}$ are complex numbers to be determined from the continuous boundary condition of atomic excitation wave function. By applying the *divide and conquer* scheme, one obtains the wave function after scattering in Region 1, which takes the following form,

$$\phi(x_1,x_2,\cdots,x_N) = \widetilde{t}_K^{(N)} e^{i(\frac{\omega_{k_1}}{v_g}x_1+\cdots+\frac{\omega_{k_N}}{v_g}x_N)}, \tag{45}$$

where the transmission coefficient for the reservoir-modified bound state, $\widetilde{t}_K^{(N)}$, is given by

$$\begin{aligned}
\widetilde{t}_K^{(N)} &= \prod_{j=1}^{N} \widetilde{t}_{k_j},\ \widetilde{t}_{k_j} = \frac{\omega_{k_j} - \Omega_j - i\Gamma/2}{\omega_{k_j} - \Omega_j + i\Gamma/2},\ j = 1, 2, \cdots, N, \quad \text{where} \\
\Omega_j =& \Omega + \mu_j, \\
\mu_j =& \sum_{i_1} \frac{\eta_{i_1}^2}{\omega_{k_j} - \omega_{a_{i_1}} + i\varepsilon} \\
&+ \sum_{n=2}^{\infty} \sum_{i_1} \sum_{i_2, i_2 \neq i_1} \cdots \sum_{i_n, i_n \neq i_{n-1}} \frac{\eta_{i_1} \beta_{i_1 i_2} \cdots \beta_{i_{n-1} i_n} \eta_{i_n}}{\prod_{l=1}^{n} (\omega_{k_j} - \omega_{a_{i_l}} + i\varepsilon)}.
\end{aligned} \tag{46}$$

To simplify $\widetilde{t}_K^{(N)}$, we now recursively invoke the continuous boundary condition of $e(x_1, \cdots, x_{N-1})$ between two adjacent regions, Region $j+1$ and Region j, for $j = 1, 2, \cdots, N$. Noting that in Region $j+1$ (*i.e.*, $x_1 < \cdots < x_j < 0 < x_{j+1} < \cdots < x_N$), e can be analytically solved for and takes the following form,

$$\begin{aligned}
e(x_1, \cdots, x_{j-1}, x_{j+1}, \cdots, x_N) = & \frac{\sqrt{N} V \prod_{l=j+1}^{N} \widetilde{t}_{k_l}}{\omega_{k_j} - \Omega_j + i\frac{\Gamma}{2}} \\
& \exp i \frac{\omega_{k_1} x_1 + \cdots + \omega_{k_{j-1}} x_{j-1} + \omega_{k_{j+1}} x_{j+1} + \cdots \omega_{k_N} x_N}{v_g}.
\end{aligned} \tag{47}$$

Likewise, in Region j (*i.e.*, $x_1 < \cdots < x_{j-2} < x_{j-1} < 0 < x_j < \cdots < x_N$), e is given by

$$\begin{aligned}
e(x_1, \cdots, x_{j-2}, x_j, \cdots, x_N) = & \frac{\sqrt{N} V \prod_{l=j}^{N} \widetilde{t}_{k_l}}{\omega_{k_{j-1}} - \Omega_{j-1} + i\frac{\Gamma}{2}} \\
& \exp i \frac{\omega_{k_1} x_1 + \cdots + \omega_{k_{j-2}} x_{j-2} + \omega_{k_j} x_j + \cdots \omega_{k_N} x_N}{v_g}.
\end{aligned} \tag{48}$$

By applying the continuous boundary condition between adjacent Region $j+1$ and j (deduced from Eq. (39b)),

$$\begin{aligned}
& e(x_1, \cdots, x_{j-2}, 0^-, x_{j+1}, \cdots, x_N) = \\
& e(x_1, \cdots, x_{j-2}, 0^+, x_{j+1}, \cdots, x_N),
\end{aligned} \tag{49}$$

one obtains

$$\omega_{k_j} - \omega_{k_{j-1}} = \mu_j - \mu_{j-1} + i\Gamma, \quad j = 2, \cdots, N. \tag{50}$$

Such $N-1$ relations and the energy conservation constraint $\sum_{j=1}^{N} \omega_{k_j} = K v_g$ uniquely determine the photon frequencies for the reservoir-modified bound state in the following form,

$$\omega_{k_j} = \frac{K v_g}{N} - \frac{\sum_{l=1}^{N} \mu_l}{N} + \mu_j + i\frac{2j - (N+1)}{2}\Gamma, \quad j = 1, 2, \cdots, N. \tag{51}$$

Thus, $\widetilde{t}_K^{(N)}$ can be simplified using Eq. (51) in the following

$$\widetilde{t}_K^{(N)} = \frac{\omega_{k_1} - \Omega_1 - i\Gamma/2}{\omega_{k_N} - \Omega_N + i\Gamma/2}. \tag{52}$$

Noting that in Eq. (51), since all μ_j's ($j = 1, \cdots, N$) and all ω_{k_j}'s are mutually dependent, the explicit expressions of ω_{k_j} do not exist. Recall that in the reservoir-free case, $t_K^{(N)} = (Kv_g - N\Omega - iN^2\Gamma/2)/(Kv_g - N\Omega + iN^2\Gamma/2)$. $\widetilde{t}_K^{(N)}$ reduces to $t_K^{(N)}$ in the absence of the reservoir. Specifically, in the absence of the reservoir (*i.e.*, $\eta = \beta = 0$), $\omega_{k_1} = Kv_g/N - i(N-1)\Gamma/2$, $\omega_{k_N} = Kv_g/N + i(N-1)\Gamma/2$, and $\Omega_1 = \Omega_N = \Omega$. By plugging such relations into Eq. (52), $\widetilde{t}_K^{(N)}$ reduces to $t_K^{(N)}$. The complex frequencies can be determined through the same procedures as those in the two-photon case, which yield $\omega_{k_1} = \xi_1 Kv_g/N - i(N-1)\Gamma\nu_1/2$, $\omega_{k_2} = \xi_2 Kv_g/N - i(N-3)\Gamma\nu_2/2$, $\cdots$, $\omega_{k_N} = \xi_N Kv_g/N + i(N-1)\Gamma\nu_N/2$. Here, $\xi_1, \cdots, \xi_N$, $\nu_1, \cdots, \nu_N$ are dimensionless real numbers, and should satisfy the following constraints: $\sum_{j=1}^N \xi_j = N$, and $\sum_{j=1}^N [N - 1 - 2(j-1)]\,\nu_j = 0$, wherein the constraints here are equivalent conditions to Eq. (51) and the energy conservation condition. With explicit expressions of $\omega_{k_1}, \omega_{k_2}, \cdots, \omega_{k_N}$ as outlined above, the in-state wave function (Eq. (44)) now reads as

$$\begin{aligned}
&\phi(x_1, \cdots, x_N) = \exp\left[iK\widetilde{x}_c - \frac{\kappa}{2}\sum_{m<n}\lambda_m|x_m - x_n|\right], \quad \text{where} \\
&\widetilde{x}_c = \sum_{j=1}^N \frac{\xi_j x_j}{N}, \quad \lambda_1 = \nu_1, \\
&\lambda_j = \sum_{l=1}^{j-1}\frac{\lambda_l}{N-j} + \frac{(N-2j+1)\nu_j}{N-j}, \ j = 2, \cdots, N-1.
\end{aligned} \tag{53}$$

Based on Eq. (53), one can construct the normalized reservoir-modified N-photon bound state $|D_K\rangle$ in the following form

$$\begin{aligned}
|D_K\rangle &= \int\cdots\int\prod_{l=1}^N dx_l D_K(x_1, \cdots, x_N)\frac{1}{\sqrt{N!}}\prod_{m=1}^N c_e^\dagger(x_m), \quad \text{where} \\
D_K(x_1, \cdots, x_N) &= \sqrt{\frac{\prod_{l=1}^{N-1}\lambda_l\kappa^{N-1}(N-1)!}{2N\pi}}e^{iK\widetilde{x_c} - \frac{\kappa}{2}\sum_{m<n}\lambda_m|x_m - x_n|},
\end{aligned} \tag{54}$$

which is an eigenstate of $\mathbf{S}^r_{e^{(N)}}$ such that $\mathbf{S}^r_{e^{(N)}}|D_K\rangle = \widetilde{t}_K^{(N)}|D_K\rangle$. In contrast to the reservoir-free N-photon bound state ($B_K(x_1, \cdots, x_N) \propto e^{iKx_c - \kappa\sum_{m<n}|x_m - x_n|/2}$), the reservoir-modified bound state has a modified inter-photon correlation width $1/\kappa \to 1/\kappa\lambda_j$ and a modified N-photon center position of $x_c \to \widetilde{x}_c$. By applying the Fourier transform on $D_K(x_1, \cdots, x_N)$

from the real space to the momentum space ($i.e.$, $D_K(k_1,\cdots,k_N)=\int\cdots\int\prod_{l=1}^{N}x_l D_K(x_1,\cdots,x_N)\frac{e^{-i\sum_{m=1}^{N}k_m x_m}}{(2\pi)^{N/2}}$), one can show that $D_K(k_1,\cdots,k_N)\propto\delta(K-\sum_{l=1}^{N}k_l)$, indicating once again the frequency anti-correlation in the reservoir-modified N-photon bound state.

Note for the reservoir-modified bound state, neither the interacting eigenstates for the restricted system variables ($i.e.$, ϕ and e), nor the transmission coefficient ($\widetilde{t}_K^{(N)}$) can be described by a simple frequency renormalization of the results in the reservoir-free case (see Eqs. (19), (A28), and (A29) in Ref. [25]). Furthermore, the reservoir-modified N-photon hybrid states can be determined through a similar procedure, and it is also found that the hybrid states can not be obtained by a frequency renormalization of the results in the reservoir-free case. Thus, the existence of the reservoir-modified bound state and the hybrid states make the reduced Hamiltonian approach invalid in the N-photon case.

D. Weak-reservoir Condition

Similar to the two-photon case, here we also provide the weak-reservoir condition for the reduced Hamiltonian approach to be approximately valid in the N-photon case when the reservoir is present. Such a weak-reservoir condition states that: first, the system-reservoir coupling $\bar{\eta}$ and secondary scattering strength $\bar{\beta}$ are both weak enough ($i.e.$, $\bar{\eta},\bar{\beta}\ll\Omega,\Gamma$); secondly, the reservoir-photon detuning is much larger than the photon-atom interaction strength, $i.e.$, $\bar{\delta}\gg(N-1)\Gamma/2$. Similar to the two-photon case, when both criteria are fulfilled, the photon frequencies of the reservoir-modified bound state are approximated by $\omega_{k_1}\approx\Omega-i(N-1)\Gamma/2,\omega_{k_2}\approx\Omega-i(N-3)\Gamma/2,\cdots,\omega_{k_N}\approx\Omega+i(N-1)\Gamma/2$ and it follows that $\mu_1\approx\mu_2\cdots\approx\mu_N\approx\alpha$, $\Omega_1\approx\Omega_2\cdots\approx\Omega_N\approx\bar{\Omega}$. It is worth noting that when both criteria are fulfilled, $\bar{\beta}\bar{D}\Delta\omega/\bar{\delta}\ll1$ also holds such that the frequency renormalization can be approximated by its first-order term ($i.e.$, $\alpha\approx\alpha_1$). The result implies that when the weak-reservoir condition holds, the interacting eigenstates for the restricted system variables ($i.e.$, $\phi(x_1,\cdots,x_N)$ and $e(x_1,\cdots,x_{N-1})$) are renormalized, which can be described by a frequency renormalization ($\Omega\to\bar{\Omega}$). When the weak-reservoir condition holds, it can be similarly shown that the solution for the reservoir-modified hybrid states now can be obtained by renormalizing the atomic transition frequency in the reservoir-free case ($\Omega\to\bar{\Omega}$).

To sum it up, when the weak-reservoir condition holds, the interacting eigenstate solutions of the restricted system variables for the extended state, bound state, and hybrid states can

be obtained by a frequency renormalization ($\Omega \to \bar{\Omega}$) from the reservoir-free results, which immediately indicates the validity of the reduced Hamiltonian approach for the N-photon Fock state transport, when the weak-reservoir condition holds. The same conclusions also apply to the N-photon two-mode case.

VI. DENSITY MATRIX APPROACH

In this section, we compare our approach with the density matrix approach. The density matrix approach provides a probabilistic measure of the system dynamics while does not directly provide the information of the photonic wave function and the entanglement. To illustrate this point, here we first use a concrete but simple example of atomic spontaneous decay into the reservoir to show that the density matrix approach yields a mixed-state solution. The procedures below follow those in Ref. [2]. The system of interest here is the atom, denoted by A, and described by the Hamiltonian, $H_A/\hbar = \omega_e a_e^\dagger a_e + \omega_g a_g^\dagger a_g$. The external reservoir and the atom-reservoir interaction are still described by H_R (Eq. (2)) and H_{SR} (Eq. (3)), respectively. The Hamiltonian that characterizes the combined system, H_{AR}, is $H_A + H_R + H_{SR}$, which is further written as $H_o(\text{free}) + H_I(\text{interaction})$, where

$$\begin{aligned}\frac{H_o}{\hbar} =&\omega_e a_e^\dagger a_e + \omega_g a_g^\dagger a_g + \sum_j [(\omega_{e_j} - i\varepsilon) a_{e_j}^\dagger a_{e_j} + \omega_{g_j} a_{g_j}^\dagger a_{g_j}],\\ \frac{H_I}{\hbar} =&\sum_j \eta_j (\sigma_{j+}\sigma_- + \sigma_+\sigma_{j-}) + \sum_{j,l,j\neq l} \frac{\beta_{jl}}{2}(\sigma_{j+}\sigma_{l-} + \sigma_{l+}\sigma_{j-}).\end{aligned} \tag{55}$$

H_I in the interaction picture, $\mathcal{V}(t)$, is

$$\begin{aligned}\mathcal{V}(t) =&e^{iH_o t/\hbar} H_I e^{-iH_o t/\hbar}\\ =&\sum_j \eta_j (e^{i(\omega_{a_j} - \Omega - i\varepsilon)t}\sigma_{j+}\sigma_- + e^{-i(\omega_{a_j} - \Omega - i\varepsilon)t}\sigma_+\sigma_{j-})\\ &+ \sum_{j,l,j\neq l} \frac{\beta_{jl}}{2}(e^{i(\omega_{a_j} - \omega_{a_l})t}\sigma_{j+}\sigma_{l-} + e^{-i(\omega_{a_j} - \omega_{a_l})t}\sigma_{l+}\sigma_{j-}).\end{aligned} \tag{56}$$

By invoking the Markovian assumptions as in Ref. [2], the density matrices obey $\rho_{AR}(t_i) = \rho_A(t_i) \otimes \rho_R(t_i)$, where ρ_A, ρ_R, and ρ_{AR} are density matrices for the atom, reservoir, and the combined system, respectively. that is, at the initial time of t_i, the atom and the external reservoir are unentangled. Thus, the equation of motion for the reduced density operator

ρ_A is

$$\begin{aligned}\dot{\rho}_A(t) =& -\frac{i}{\hbar}\mathrm{Tr}_R[\mathcal{V}(t), \rho_A(t_i)\otimes\rho_R(t_i)] \\ & -\frac{1}{\hbar^2}\mathrm{Tr}_R\int_{t_i}^{t} dt'[\mathcal{V}(t),[\mathcal{V}'(t),\rho_A(t')\otimes\rho_R(t_i)]].\end{aligned} \tag{57}$$

By inserting Eq. (56) into Eq. (57), the terms that yield non-vanishing results on the right-hand side of Eq. (57), are given by

$$\begin{aligned}&\sum_{j,l}\eta_j\eta_l\int_{t_i}^{t}dt'\Big\{e^{i(\omega_{a_j}-\Omega-i\varepsilon)t-i(\omega_{a_l}-\Omega-i\varepsilon)t'}\mathrm{Tr}_R[\sigma_{j+}\sigma_{l-}\rho_R(t_i)] \\ &[\sigma_-\sigma_+\rho_A(t') - \sigma_+\rho_A(t')\sigma_-] + e^{-i(\omega_{a_j}-\Omega-i\varepsilon)t+i(\omega_{a_l}-\Omega-i\varepsilon)t'} \\ &\mathrm{Tr}_R[\sigma_{j-}\sigma_{l+}\rho_R(t_i)][\sigma_+\sigma_-\rho_A(t') - \sigma_-\rho_A(t')\sigma_+] + h.c.\Big\},\end{aligned} \tag{58}$$

where $h.c.$ denotes the hermitian conjugate. Assuming that no oscillators are excited initially, the initial state of the reservoir at t_i is described by $|\psi\rangle = |g_1\rangle|g_2\rangle\cdots$, and its density matrix is $\rho_R(t_i) = |\psi\rangle\langle\psi|$, where $|g_j\rangle$ ($|e_j\rangle$) denotes that the j-th oscillator is at the ground (excited) state. We now apply the fermionic algebra $\{\sigma_{j-},\sigma_{l+}\} = \delta_{jl}$ ($\{\}$ denotes the anti-commutator), and employ the identity of $\mathrm{Tr}_R[\sigma_{j+}\sigma_{l-}\rho_R(t_i)] = \langle\psi|\sigma_{j+}\sigma_{l-}|\psi\rangle = 0$ in Eq. (58). The right-hand side of Eq. (57) is simplified as

$$\begin{aligned}\dot{\rho}_A(t) =& -\sum_j\eta_j^2\int_{t_i}^{t}dt'e^{-i(\omega_{a_j}-\Omega-i\varepsilon)(t-t')} \\ & [\sigma_+\sigma_-\rho_A(t') - \sigma_-\rho_A(t')\sigma_+] + h.c.\end{aligned} \tag{59}$$

Similar to Eq. (9), we now convert Eq. (59) to the continuum limit and get

$$\begin{aligned}\dot{\rho}_A(t) =& -\int_0^\infty d\omega\eta^2(\omega)D(\omega)\int_{t_i}^{t}dt'e^{-i(\omega-\Omega-i\varepsilon)(t-t')} \\ & [\sigma_+\sigma_-\rho_A(t') - \sigma_-\rho_A(t')\sigma_+] + h.c.\end{aligned} \tag{60}$$

Noting that $D(\omega)|_{\omega<0} = 0$, we now extend the lower limit of the integral by $\int_0^\infty d\omega \to \int_{-\infty}^\infty d\omega$. Then, similar to the Weisskopf-Wigner theory, we approximate $\eta^2(\omega)D(\omega)$ using the value when ω is around the atomic transition frequency Ω, and invoke the identity $\int_{-\infty}^\infty e^{-i(\omega-\Omega-i\varepsilon)(t-t')}d\omega = 2\pi\delta(t-t')$ and $\int_{t_i}^t\delta(t-t')dt' \approx \frac{1}{2}\int_{-\infty}^\infty dt'\delta(t-t')$, to yield the following equation

$$\dot{\rho}_A = -\gamma_D[\sigma_+\sigma_-\rho_A - 2\sigma_-\rho_A\sigma_+ + \rho_A\sigma_+\sigma_-], \tag{61}$$

where $\gamma_D = \pi\eta^2(\Omega)D(\Omega)$ is the resulting dissipation rate. The right-hand side of Eq. (61) is exactly the Lindblad superoperator with a damping rate γ_D.

By applying Eq. (61) to the case of atomic spontaneous decay into the reservoir, the dynamics for the reduced density matrix is given by

$$\rho_A = \begin{bmatrix} \rho_{ee} & \rho_{eg} \\ \rho_{ge} & \rho_{gg} \end{bmatrix}, \quad \begin{cases} \dot{\rho}_{ee} = -2\gamma_D \rho_{ee}, \\ \dot{\rho}_{eg} = -\gamma_D \rho_{eg}, \\ \dot{\rho}_{gg} = 2\gamma_D \rho_{ee}, \end{cases} \tag{62}$$

where ρ_{ee} and ρ_{gg} are the probabilities of being at the excited and ground states, respectively; ρ_{eg} and ρ_{ge} represent the transition probabilities from excited state to the ground state and the reverse process. To satisfy the initial condition that the atom is initially at the excited state, *i.e.*, $\rho_{ee}(0) = 1$, $\rho_{eg}(0) = 0$, and $\rho_{gg}(0) = 0$, the solutions to Eq. (62) are obtained by $\rho_{ee}(t) = e^{-2\gamma_D t}$, $\rho_{eg}(t) = 0$, and $\rho_{gg}(t) = 1 - e^{-2\gamma_D t}$. It can be straightforwardly checked that this is not a pure-state solution.

Next, we compare the results of the reservoir-induced photonic dissipation between those using the Markovian density matrix and those using the entanglement-preserving approach. First, the dissipation rate γ_D obtained in Eq. (61), the Lindblad superoperator for the density operator, is the same as *the lowest-order* dissipation rate γ_1 in Eq. (10) in our entanglement-preserving approach, as the density matrix approach does not describe the photonic dynamics in the reservoir (*i.e.*, the coherent hopping events described by the β's). That is, for coherent processes, only in the weak-reservoir limit ($\bar{\beta}\bar{D}\Delta\omega/\bar{\delta} \ll 1$), does the density matrix approach yields the approximate dissipation rate. Nonetheless, the frequency shift Δ_1 is not predicted by the density matrix approach even in the weak-reservoir limit. Our approach provides a framework to investigate the photonic loss mechanisms by engineering the excitable reservoir and beyond the weak-reservoir limit.

As a further comparison, we now apply the *non-Markovian* density matrix approach to investigate the same excitable reservoir scenario (Hamiltonian described by Eq. (56)). Our results show that although the non-Markovian approach can readily describe the effects of dissipations up to an arbitrary order of accuracy but it does not provide information of multi-photon entanglement, and again only yields a mixed state solution [28]. Notably, the non-Markovian condition requires that the system and the reservoir are initially entangled, i.e., the general system-reservoir state is described by $|\Psi_{AR}(t)\rangle = a_o|g\rangle\otimes|g_1\rangle|g_2\rangle\cdots + a(t)|e\rangle\otimes|g_1\rangle|g_2\rangle\cdots + \sum_j b_j(t)|g\rangle\otimes|g_1\rangle|g_2\rangle\cdots|e_j\rangle\cdots$ where $|e\rangle$ ($|g\rangle$) is atomic excited (ground) state and $|e_j\rangle$ ($|g_j\rangle$) is defined the same as the Markovian approach. a_o, a, and b_j are wave

function amplitudes for ground, atomic excited, and reservoir excited states, respectively. By applying the Schrödinger equation, i.e., $i\hbar\partial_t|\Psi_{AR}(t)\rangle = \mathcal{V}(t)|\Psi_{AR}(t)\rangle$, one obtains the following equations of motion to describe the wave function evolution

$$\dot{a}(t) = -i\sum_j \eta_j b_j(t) e^{-i(\omega_{a_j}-\Omega-i\varepsilon)t}, \tag{63a}$$

$$\dot{b}_j(t) = -i\eta_j a(t) e^{i(\omega_{a_j}-\Omega-i\varepsilon)t} - i\sum_{l,l\neq j}\beta_{jl} e^{i(\omega_{a_j}-\omega_{a_l})t} b_l(t),\ j=1,2,\cdots, \tag{63b}$$

subject to the initial condition: the atom is fully excited at initial time t_i, i.e., $a(t_i) = 1,\ b_j(t_i) = 0$. By definition, the combined density matrix is $\rho_{AR}(t) = |\Psi_{AR}(t)\rangle\langle\Psi_{AR}(t)|$. The reduced density matrix ρ_A can be further acquired by tracing over reservoir degrees of freedom, i.e., $\rho_A = \mathrm{Tr}_R[\rho_{AR}] = \sum_{|r\rangle}\langle r|\rho_{AR}|r\rangle$ where a complete set of reservoir eigenstates $\{|r\rangle\}$ includes the reservoir ground state $|r_o\rangle = |g_1\rangle|g_2\rangle\cdots$ and singly-excited states $|r_j\rangle = |g_1\rangle|g_2\rangle\cdots|e_j\rangle\cdots$. It can be shown that ρ_A fulfills

$$\dot{\rho}_A(t) = -i\Delta_{NM}(t)\left[\sigma_+\sigma_-, \rho_A(t)\right] - \gamma_{NM}(t)\left[\sigma_+\sigma_-\rho_A(t) + \rho_A(t)\sigma_+\sigma_- - 2\sigma_-\rho_A(t)\sigma_+\right], \tag{64a}$$

$$\Delta_{NM}(t) = -\mathrm{Im}\left[\frac{\dot{a}(t)}{a(t)}\right], \quad \gamma_{NM}(t) = -\mathrm{Re}\left[\frac{\dot{a}(t)}{a(t)}\right], \tag{64b}$$

$$\begin{aligned}\dot{a}(t) =& (-i)^2\sum_{i_1}\eta_{i_1}^2 e^{-i(\omega_{a_{i_1}}-\Omega-i\varepsilon)t}\int_{t_i}^{t} a(t_1)e^{i(\omega_{a_{i_1}}-\Omega-i\varepsilon)t_1}dt_1 \\ &+\sum_{n=2}^{\infty}(-i)^{n+1}\sum_{i_1}\sum_{i_2\neq i_1}\cdots\sum_{i_n\neq i_{n-1}}\eta_{i_1}\beta_{i_1 i_2}\cdots\beta_{i_{n-1}i_n}\eta_{i_n}e^{-i(\omega_{a_{i_1}}-\Omega-i\varepsilon)t}\times \\ &\int_{t_i}^{t} e^{i(\omega_{a_{i_1}}-\omega_{a_{i_2}})t_1}dt_1\cdots\int_{t_i}^{t_{n-2}} e^{i(\omega_{a_{i_{n-1}}}-\omega_{a_{i_n}})t_{n-1}}dt_{n-1}\int_{t_i}^{t_{n-1}} a(t_n)e^{i(\omega_{a_{i_n}}-\Omega-i\varepsilon)t_n}dt_n,\end{aligned} \tag{64c}$$

where $\Delta_{NM}(t)$ and $\gamma_{NM}(t)$ are time-dependent frequency shift and dissipation rate for non-Markovian approach, respectively. Eq. (64c) is obtained by recursively integrating and substituting Eq. (63b) in Eq. (63a) to eliminate b_j. Apparently, such a non-Markovian approach can describe photon hopping processes up to an arbitrary order of accuracy. Moreover, such a approach does not apply when multi-photon entanglement is necessarily taken into account, e.g., N-photon bound state solution in Sec. V. The comparison of the Markovian, the non-Markovian density matrix approaches, and the entanglement-preserving approach is summarized in Table II.

TABLE II. Comparison of Markovian and non-Markovian density matrix (DM) approach and the entanglement-preserving approach.

	Markovian DM	non-Markovian DM	Entanglement-Preserving
order of accuracy	lowest-order	all-order	all-order
multi-photon entanglement	×	×	√
state description	mixed state	mixed state	pure state

VII. CONCLUSION AND OUTLOOK

In this article, we present a comprehensive study on the effects of reservoir-induced dissipation for an arbitrary photonic Fock state transport in wQED systems. Specifically, using the entanglement-preserving approach, we rigorously validate the reduced Hamiltonian approach in the single-photon case, wherein the Hamiltonian is renormalized by an added complex number $\Delta - i\gamma$ in the atomic transition frequency. For the multi-photon case, we show that the photon transport, in general, can not be described by a reduced Hamiltonian approach. In addition, we also identify a weak-reservoir condition such that, when it holds, the multi-photon transport can still be described by the reduced Hamiltonian approach.

In essentially all quantum optical scenarios, photonic dissipation results from both photonic scattering loss (coupling with a non-excitable reservoir) and material loss (coupling with an excitable reservoir). For photonic scattering loss, it has been shown that, for all input states, the effects can be incorporated by adding an imaginary part $-i\gamma_S$ in the renormalized transition frequency (γ_S is the photonic scattering loss rate) [8]. Thus, when the weak-reservoir condition is satisfied, to take into account the effects of both scattering loss and material loss, the reduced Hamiltonian approach is valid via the frequency renormalization $\Omega \to \Omega + \Delta - i(\gamma + \gamma_S)$. As a coherent state is a linear superposition of Fock states, the reduced Hamiltonian approach is also valid when the input is a coherent state under the weak-reservoir condition. Moreover, by employing the explicit photon-cavity interactions, and applying the same approach outlined above, it can be shown that the reduced Hamiltonian approach is also valid in the presence of cavity dissipations. That is, the dissipation rate γ due to the reservoir can be measured by a single-photon scattering experiment (e.g., a transmission measurement); the resulting reduced Hamiltonian is then valid for all quantized

optical input.

An example of the excitable reservoirs could be, for example, a layer of doped semiconductor coupled to a photonic waveguide at cryogenic temperatures. The dissipation rate can be altered via changing the doping concentration. On the other hand, with the advent of advanced nano-fabrication technologies, we speculate that the reservoir could be engineered so that the weak-reservoir condition is no longer satisfied. One possibility is an engineered excitable reservoir consisting of optical cavities as the oscillators. The number and the placement of the optical cavities determine the various interaction strengths and, more importantly, the admissible closed paths for the hopping photons. For an engineered excitable reservoir, the dissipation rate obtained from a single-photon scattering experiment is inadequate to predict the precise quantum dynamics for an input of a correlated photonic state (*e.g.*, a two-photon bound state).

Our results provide a tremendous convenience for both analytical investigations and numerical modelings of correlated few-photon transport in wQED systems in the dissipative regime [29, 30], and can be generalized to more complicated wQED architectures [31–33]. Moreover, our results also provide valuable insights on the studies of effects of dissipation in quantum many-body systems [34–36].

ACKNOWLEDGMENTS

This work was supported in part by National Science Foundation ECCS Grant No. 1608049 and 1541617.

---

[1] R. Feynman, *Statistical Mechanics: A Set Of Lectures* (Avalon Publishing, 1998).

[2] M. O. Scully and M. S. Zubairy, *Quantum Optics* (Cambridge university press, 1997).

[3] G. Lindblad, Communications in Mathematical Physics **48**, 119 (1976).

[4] C. W. Gardiner and M. J. Collett, Phys. Rev. A **31**, 3761 (1985).

[5] P. Zoller, M. Marte, and D. F. Walls, Phys. Rev. A **35**, 198 (1987).

[6] J. Dalibard, Y. Castin, and K. Mølmer, Phys. Rev. Lett. **68**, 580 (1992).

[7] J.-T. Shen and S. Fan, Phys. Rev. A **79**, 023837 (2009).

[8] Z. Chen, Y. Zhou, and J.-T. Shen, Opt. Lett. **42**, 887 (2017).

[9] C. Sirtori, J. Faist, F. Capasso, D. L. Sivco, A. L. Hutchinson, and A. Y. Cho, Applied Physics Letters **66**, 3242 (1995).

[10] J. D. Joannopoulos, S. G. Johnson, J. N. Winn, and R. D. Meade, *Photonic crystals: molding the flow of light* (Princeton university press, 2011).

[11] S. K. Selvaraja, E. Sleeckx, M. Schaekers, W. Bogaerts, D. V. Thourhout, P. Dumon, and R. Baets, Optics Communications **282**, 1767 (2009).

[12] H. Lee, T. Chen, J. Li, K. Y. Yang, S. Jeon, O. Painter, and K. J. Vahala, Nature Photonics **6**, 369 (2012).

[13] J.-T. Shen and S. Fan, Phys. Rev. Lett. **95**, 213001 (2005).

[14] C. Gonzalez-Ballestero, E. Moreno, and F. J. Garcia-Vidal, Phys. Rev. A **89**, 042328 (2014).

[15] Q. Li, L. Zhou, and C. P. Sun, Phys. Rev. A **89**, 063810 (2014).

[16] G. Calajó, F. Ciccarello, D. Chang, and P. Rabl, Phys. Rev. A **93**, 033833 (2016).

[17] M. P. Schneider, T. Sproll, C. Stawiarski, P. Schmitteckert, and K. Busch, Phys. Rev. A **93**, 013828 (2016).

[18] I. M. Mirza and J. C. Schotland, Phys. Rev. A **94**, 012302 (2016).

[19] Z. Liao, X. Zeng, H. Nha, and M. S. Zubairy, Physica Scripta **91**, 063004 (2016).

[20] L. Davidovich, M. Brune, J. M. Raimond, and S. Haroche, Phys. Rev. A **53**, 1295 (1996).

[21] M. Neeley, M. Ansmann, R. C. Bialczak, M. Hofheinz, N. Katz, E. Lucero, A. O'Connell, H. Wang, A. N. Cleland, and J. M. Martinis, Phys. Rev. B **77**, 180508 (2008).

[22] F. Beaudoin, J. M. Gambetta, and A. Blais, Phys. Rev. A **84**, 043832 (2011).

[23] A. González-Tudela, V. Paulisch, D. E. Chang, H. J. Kimble, and J. I. Cirac, Phys. Rev. Lett. **115**, 163603 (2015).

[24] J.-T. Shen and S. Fan, Physical Review Letters **98**, 153003 (2007).

[25] Y. Shen and J.-T. Shen, Phys. Rev. A **92**, 033803 (2015).

[26] J.-T. Shen and S. Fan, Phys. Rev. A **76**, 062709 (2007).

[27] O. Firstenberg, T. Peyronel, Q.-Y. Liang, A. V. Gorshkov, M. D. Lukin, and V. Vuletic, Nature **502**, 71 (2013).

[28] H.-P. Breuer and F. Petruccione, *The theory of open quantum systems* (Oxford University Press on Demand, 2002).

[29] K. Lalumière, B. C. Sanders, A. F. van Loo, A. Fedorov, A. Wallraff, and A. Blais, Phys. Rev. A **88**, 043806 (2013).

[30] Z. Chen, Y. Zhou, and J.-T. Shen, Phys. Rev. A **96**, 053805 (2017).

[31] D. Roy, Phys. Rev. Lett. **106**, 053601 (2011).

[32] Y. Zhou, Z. Chen, and J.-T. Shen, Phys. Rev. A **95**, 043832 (2017).

[33] Y. Lu, S. Gao, A. Fang, P. Li, F. Li, and M. S. Zubairy, Opt. Express **25**, 16151 (2017).

[34] N. Syassen, D. M. Bauer, M. Lettner, T. Volz, D. Dietze, J. J. García-Ripoll, J. I. Cirac, G. Rempe, and S. Dürr, Science **320**, 1329 (2008).

[35] I. Carusotto, D. Gerace, H. E. Tureci, S. De Liberato, C. Ciuti, and A. Imamoğlu, Phys. Rev. Lett. **103**, 033601 (2009).

[36] F. Brennecke, R. Mottl, K. Baumann, R. Landig, T. Donner, and T. Esslinger, Proceedings of the National Academy of Sciences **110**, 11763 (2013).